THE UNIVERSITY OF GRONINGEN

BACHELOR THESIS

Simple molecules in the inner regions of protoplanetary disk models

Author:
Jelke Bethlehem

Supervisor:
prof. dr. I.E.E. (Inga) Kamp

A thesis submitted in fulfillment of the requirements for the degree of Bachelor of Astronomy

November 30, 2018

THE UNIVERSITY OF GRONINGEN

Abstract

Kapteyn Astronomical Institute
Faculty of Science and Engineering

Bachelor of Astronomy

Simple molecules in the inner regions of protoplanetary disk models

by Jelke Bethlehem

The chemical species in a protoplanetary disk react with each other. In the inner part of a protoplanetary disk molecules like ethyn(C_2H_2), methane(CH_4) and hydrogen cyanide(HCN) are constantly formed and destroyed. The aim of this theoretical study is to understand why there is a difference in the relative abundance for C_2H_2, CH_4 and HCN between two protoplanetary disk models. These models are ProDiMo and a model made by Agúndez et al, both models claim that they are made for at typical T Tauri star. The difference between the relative abundance for C_2H_2, CH_4 and HCN between these models is of several orders of magnitude. Comparing the models will be done by comparing the chemistry, thus the species, reactions, reaction rates and also by comparing the structure like disk size, temperature, mass and grain properties. The reason for the difference turned out to be the grain sizes for the surface of the disk and the timescales for the midplane of disk.

Contents

Chapter 1

Aim of the thesis

Protoplanetary disk models play a key role in understanding the process of planet formation. From observations in the near and mid-IR wavelengths we know that there exist simple organic molecules such as acetylene (C_2H_2), hydrogen cyanide (HCN) and methane (CH_4) in protoplanetary disks (Lahuis et al., 2006)(Salyk et al., 2011). The reason for choosing these three molecules is because these are Strong in mid-IR spectra of the disks. This gives a reason to understand their formation and destruction. By zooming in on the inner 3 AU of the protoplanetary disk model called ProDiMo (Woitke, P., Kamp, I., and Thi, W.-F., 2009) a thermo-chemical disk model around a TTauri star. The chemical abundances of these three key species in this model deviate thirteen orders of magnitude in the surface from a model used by Agúndez et al. (2008) which is also for a T Tauri star. This difference is found in the relative abundance of C_2H_2, CH_4 and HCN. In ProDiMo the relative abundances of $10^{-4} - 10^{-5}$ are found in the midplane, while in the the paper by Marcelino Agúndez the high relative abundance is higher up in the disk close to the surface as shown in figure 1.1.

The aim of this thesis is to investigate what causes the difference in relative abundance for C_2H_2, CH_4 and HCN between the models for a TTauri protoplanetary disk from ProDiMo (Woitke, P., Kamp, I., and Thi, W.-F., 2009) and Agúndez et al. (2008), Agúndez et al. (2018).

This difference might be due to a different chemical network or a fundamental difference in the disk model. In this research I will compare various parts of the models with each other in order to determine the factor that causes this major difference. These various parts are the species, chemical reactions, reaction rates and temperatures at which the reactions occur. Furthermore also the parameters of the disk model such as disk mass, disk radius, dust composition, grain size, gas to dust ratio and cosmic ray ionization rate of H_2 will be discussed and compared.

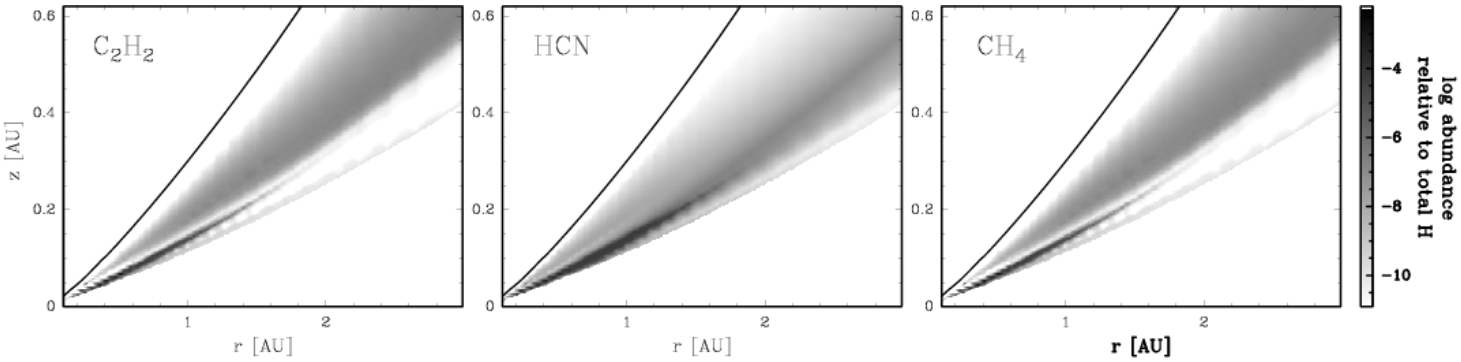

(A) Figure 3 from Agúndez et al. (2008)

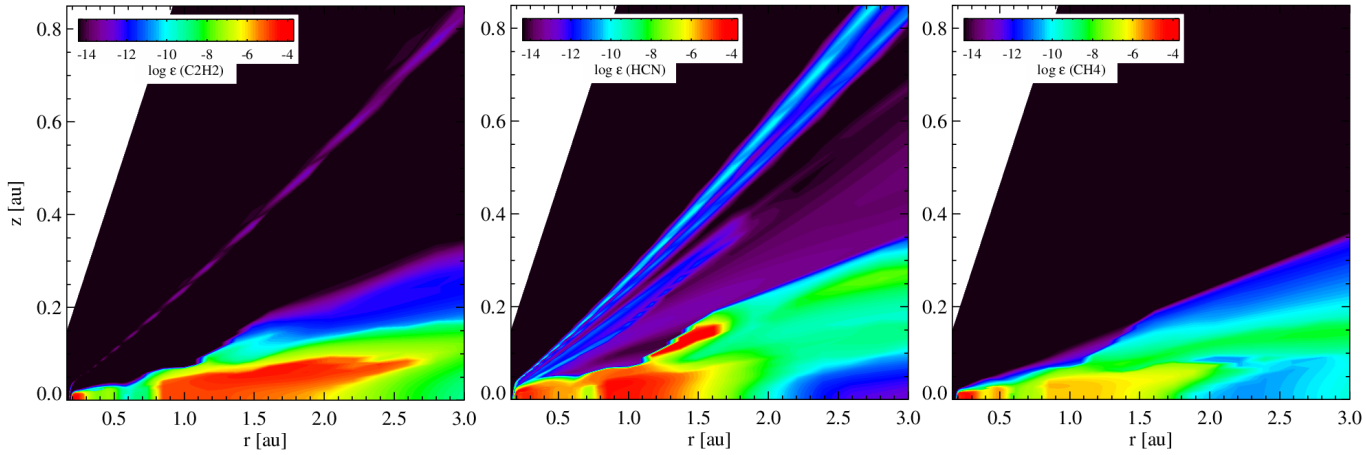

(B) Results of ProDiMo

FIGURE 1.1: Relative abundance of C_2H_2, CH_4 and HCN with respect to total H as a function of the height in the disk

Agúndez et al. produced very recently a new paper with an upgraded model (Agúndez et al., 2018). In this model the same difference with the ProDiMo model still exists. The relative abundances are shown in figure 1.2. In these figures there is an abundance of roughly 10^{-5} for C_2H_2, CH_4 and HCN between a radius of 0.5 and 1 AU.

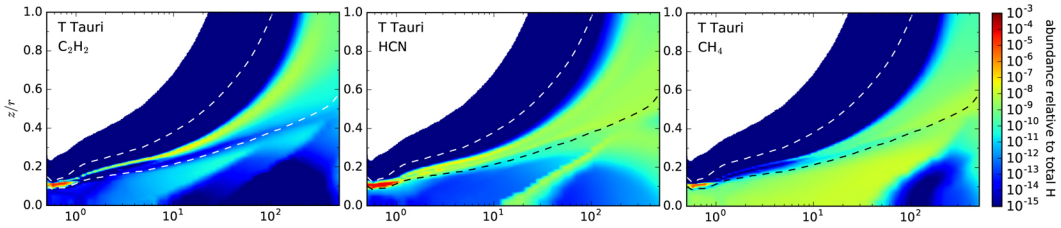

FIGURE 1.2: Relative abundance as produced by the new model of Agúndez et al., taken from figure 6 from Agúndez et al. (2018)

Chapter 2

Protoplanetary disk models

2.1 Protoplanetary disk

2.1.1 Structure

A protoplanetary disk can be described as a rotating dusty gaseous system transporting a net amount of mass towards the central star and the angular momentum outward. Due to this these disks can be characterized by strong radial and vertical temperature and density gradients (Henning and Semenov, 2013). High energy radiation penetrates the upper layers of the protoplanetary disk causing processes like photo dissociation and ionization this radiation does not reach the disk midplane. In general the disk midplane is very cold causing almost all molecules to freeze out at a radius larger than 1 AU.

2.1.2 Classification

Protoplanetary disks can be classified into three different classes using the luminosity of the central star. Protoplanetary disks can be classified as disks around brown dwarfs, disks around T Tauri stars like the sun and as disks around more luminous and massive Herbig Ae/Be stars (Henning and Semenov, 2013). ProDiMo uses a sun-like T Tauri star with a mass of 0.7 solar mass. T Tauri stars are young and pre-main sequence stars. The mass in the protoplanetary disk is about 1% dust and 99% gas, which is exactly the dust to gas ratio that ProDiMo uses.

2.1.3 Dust properties

Dust in the disk heats up the disk by absorbing incoming radiation, as more light gets absorbed the disk becomes more opaque. In figure 2.1 the relation between grain properties and the absorption coefficient is plotted. In most models the total dust mass is set. This means the assumption on the grain size has a direct correlation with the opacity in the disk. For example in the second panel of figure 2.1 a maximum dust radius of 10 mm(red) and 0.1 mm(green) causes a difference of a factor 10 in the absorption coefficient at micrometer wavelengths.

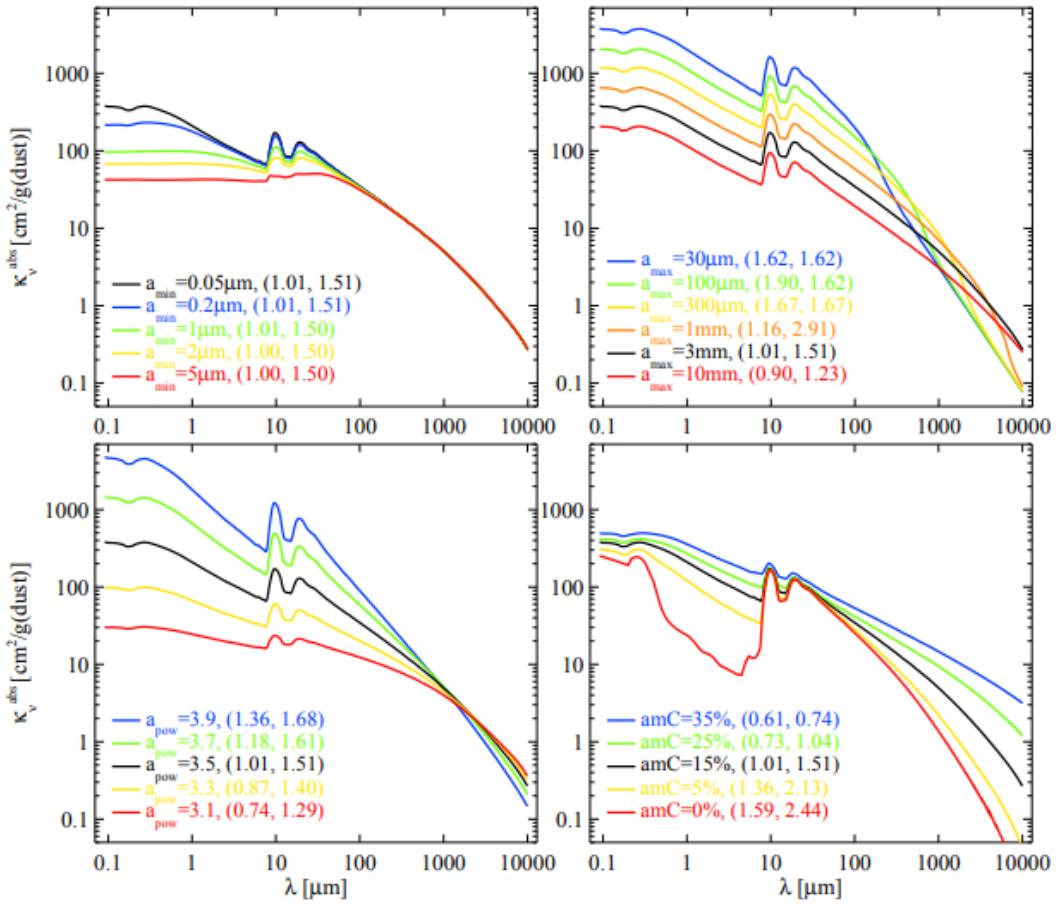

FIGURE 2.1: Dust absorption coefficient per dust mass as function of dust size and material parameters, figure 3 from Woitke et al. (2016)

2.2 ProDiMo

2.2.1 What is ProDiMo

ProDiMo is an acronym for Protoplanetary Disk Model. ProDiMo uses global iterations to calculate the physical, thermal and chemical structure of the disk. The 2D dust radiative transfer is solved once at the beginning, because for this chemistry project a simplified model will suffice. The scale height is fixed by a parametrized formula. The chemistry includes gas and photo-chemistry, Polycyclic Aromatic Hydrocarbons and X-ray chemistry. The chemical network is solved together with the gas thermal balance. The thermal balances requires all heating and cooling processes that are part of the model. ProDiMo calculates all cooling and heating processes and solves T_{gas} numerically (Woitke, P., Kamp, I., and Thi, W.-F., 2009).

2.2.2 Density structure

ProDiMo uses a power law to determine the column density

$$\Sigma(r) = \Sigma_0 r^{-\epsilon}$$

where Σ_0 is determined by the total mass of the disk

$$M_{disk} = 2\pi \int_{R_{in}}^{R_{out}} \Sigma(r) r dr$$

In these formulas R_{in} and R_{out} define the inner and outer radius of the disk. Σ_0 is the column density at an arbitrary point within R_{in} and ϵ is the scaling exponent.

The density is vertically smeared out using a Gaussian distribution, combining this with the scale height parametrized as

$$H(r) = H_0 (\frac{r}{R_{in}})^{\beta}$$

this results in the full 2D density distribution where the scale height determines the shape of the disk, leading to a flat or a flaring disk. Beta is called the flaring parameter.

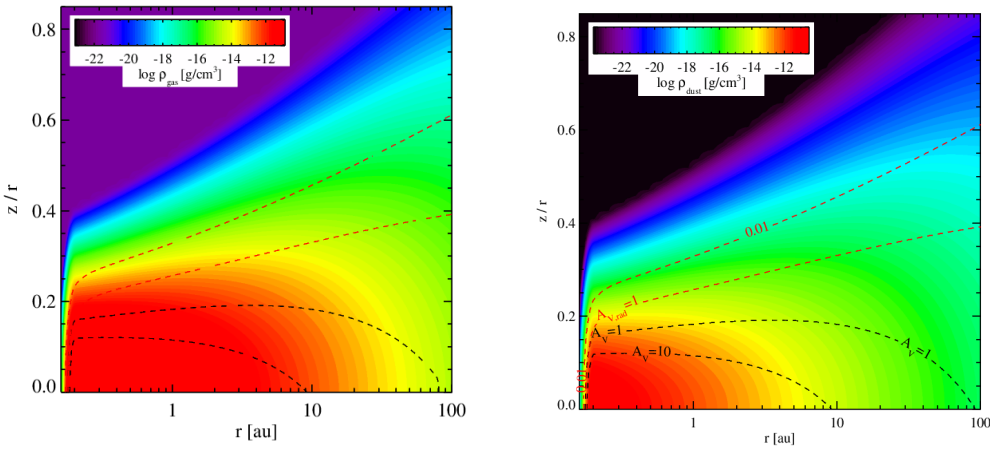

(A) gas density (B) Dust density

FIGURE 2.2: The two dashed red lines are radial extinction of 0.01 and 1 and the two black lines are the vertical extinction of 1 and 10

In figure 2.2, there is on the left side the gas mass density and on the right side the dust density. The particle density is defined as, $n_{<H>} = n_H + 2\, n_{H_2}$ the gas mass density is the particle density multiplied with the the atomic mass of hydrogen and the mean molecular weight. The mean molecular weight is 1.4. The gas mass density is a factor 100 higher than the dust mass density throughout the entire disk, because the dust to gas mass ratio is constant. From these figures it is also visible that the disk is flaring and not flat.

ProDiMo calculates the relative abundance of species as can be seen in figure 1.1. The relative C_2H_2 abundance is defined as

$$\epsilon_{C_2H_2} = \frac{n_{C_2H_2}}{n_{<H>}} = \frac{n_{C_2H_2}}{n_H + 2\, n_{H_2}}$$

this is the case for all species not just for C_2H_2.

2.2.3 Parameters of the ProDiMo model

ProDiMo does not have the stellar radius as a parameter. ProDiMo calculates this from the luminosity and effective temperature using the Stefan-Boltzmann law

$$L = 4\pi R^2 \sigma T^4$$

where σ is the Stefan-Boltzmann constant, T the effective Temperature, R the stellar radius and L the luminosity . All parameters are shown in table 2.1.

Parameter	Value
Disk	
Disk mass	0.015 $M_\odot$
Inner disk radius	0.16 au
Outer disk radius	100 au
Gas-to-dust mass ratio	100
Radial surface density power index	1.0
Dust composition	50 % silicates
	50 % graphites
Minimum dust grain radius	0.005 μm
Maximum dust grain radius	750 μm
Dust size distribution power index	3.0
Cosmic-ray ionization rate of H_2	$1.7x10^{-17}$ s^{-1}
TTauri star	
Stellar mass	0.7 $M_\odot$
Stellar radius	2.25 $R_\odot$
Stellar effective temperature	4000 K
Luminosity	1 $L_\odot$

TABLE 2.1: Parameters of the ProDiMo disk model

2.2.4 Chemistry

The chemistry is written in a modular form so that it is possible to change the selection of species and reactions (Woitke, P., Kamp, I., and Thi, W.-F., 2009). In the model used in this paper there are 235 different species of which 69 neutral species, 100 positive ions plus the negative ions H^-, PAH^-, free electrons and 63 ice molecules. These 235 species are shown in table 2.2. For the reactions the model makes use of the UMIST2012 (McElroy, D. et al., 2013) database and a database for which the rate coefficients have been collected over time. There is one crucial reaction that does not exist within UMIST2012, this is the H2 formation on dust grains. The UMIST2012 database has a total of 6225 chemical reactions and the additional file has 1555 reactions of which a large part already exist in the UMIST2012 file, if reactions exist within in both databases the UMIST2012 values are used. From these databases, 2842 reactions are called to use in our model with the respective 235 species. An interesting aspect of the model is that there are not any negative species inside it besides e^-, H^- and PAH^-. All other negative ions have not been included in order to ensure that there are no dead ends within the chemical network. ProDiMo runs the model until steady state is reached.

To calculate the rate and rate coefficients ProDiMo uses the following formulas. In the UMIST2012 and additional reaction file there are an a, b and c factor supplied,

Neutral species							
H	H_2	H_{2exc}	He	C	CH	CH_2	CH_3
CH_4	C_2	C_2H	C_2H_2	C_2H_3	C_2H_4	C_2H_5	C_3
C_3H	C_3H_2	C_4	CN	HCN	HNC	H_2CN	OCN
CO	HCO	CO_2	C_2O	H_2CO	CH_3O	CH_2OH	CH_3OH
CS	HCS	H_2CS	OCS	N	NH	NH_2	NH_3
N_2	NO	NO_2	HNO	NS	O	OH	H_2O
O_2	SO	SO_2	S	HS	H_2S	Si	SiH
SiH_2	SiH_3	SiH_4	SiC	SiN	SiO	SiS	Mg
Fe	Na	Ne	Ar	PAH			
Ions							
H^+	H^-	H_2^+	H_3^+	He^+	HeH^+	C^+	C^{++}
CH^+	CH_2^+	CH_3^+	CH_4^+	CH_5^+	C_2^+	C_2H^+	C_2H_2+
$C_2H_3^+$	$C_2H_4^+$	$C_2H_5^+$	C_3^+	C_3H^+	$C_3H_2^+$	$C_3H_3^+$	C_4^+
C_4H^+	CN^+	HCN^+	$HCNH^+$	OCN^+	CO^+	HCO^+	CO_2^+
HCO_2^+	C_2O^+	HC_2O^+	H_2CO^+	H_3CO^+	CH_3OH^+	$CH_3OH_2^+$	CS^+
HCS^+	H_2CS^+	H_3CS^+	OCS^+	$HOCS^+$	N^+	N^{++}	NH^+
NH_2^+	NH_3^+	NH_4^+	N_2^+	HN_2^+	NO^+	NO_2^+	HNO^+
H_2NO^+	NS_+	HNS^+	O^+	O^{++}	OH^+	H_2O^+	H_3O^+
O_2^+	O_2H^+	SO^+	SO_2^+	HSO_2^+	S^+	S_{++}	HS^+
H_2S^+	H_3S^+	Si^+	Si^{++}	SiH^+	SiH_2^+	SiH_3^+	SiH_4^+
SiH_5^+	SiC^+	$HCSi^+$	SiN^+	$HNSi^+$	SiO^+	$SiOH^+$	SiS^+
$HSiS^+$	Mg^+	Mg^{++}	Fe^+	Fe^{++}	Na^+	Na^{++}	Ne^+
Ne^{++}	Ar^+	Ar^{++}	PAH^-	PAH^+	PAH^{++}	PAH^{+++}	
Ices							
$Mg\#$	$Fe\#$	$Na\#$	$C\#$	$CH\#$	$CH_2\#$	$CH_3\#$	$CH_4\#$
$C_2\#$	$C_2H\#$	$C_2H_2\#$	$C_2H_3\#$	$C_2H_4\#$	$C_2H_5\#$	$C_3\#$	$C_3H\#$
$C_3H_2\#$	$C_4\#$	$CN\#$	$HCN\#$	$HNC\#$	$H_2CN\#$	$OCN\#$	$CO\#$
$HCO\#$	$CO_2\#$	$C_2O\#$	$H_2CO\#$	$CH_3O\#$	$CH_2OH\#$	$CH_3OH\#$	$CS\#$
$HCS\#$	$H_2CS\#$	$OCS\#$	$N\#$	$NH\#$	$NH_2\#$	$NH_3\#$	$N_2\#$
$NO\#$	$NO_2\#$	$HNO\#$	$NS\#$	$O\#$	$OH\#$	$H_2O\#$	$O_2\#$
$SO\#$	$SO_2\#$	$S\#$	$HS\#$	$H_2S\#$	$Si\#$	$SiH\#$	$SiH_2\#$
$SiH_3\#$	$SiH_4\#$	$SiC\#$	$SiN\#$	$SiO\#$	$SiS\#$	$PAH\#$	

TABLE 2.2: Species included in the ProDiMo model

from these the reaction rate coefficient k is calculated. This formula is only valid for two body neutral neutral reactions. In these formulas a is the pre-exponential factor, b is indicating the temperature dependency and c is the activation energy. Furthermore n_1 and n_2 indicate the abundance of the reactants. The rate coefficient is then calculated as

$$k = a(T/300)^b e^{-\frac{c}{T})}$$

and the rate becomes

$$r = k\, n_1\, n_2$$

k is the rate coefficient and r is the rate itself, k is model independent.

There are a lot of different formation channels C_2H_2, CH_4 and HCN, so it is not possible to say what the full formation pathway is for ProDiMo. However C_2H_2, CH_4 and HCN exist within the midplane it is safe to say they originate from the reaction with H_2, because there is no free H in the midplane and these species must

react with H or H_2 in order to form. As shown in figure 1.1 ProDiMo has a very low relative abundance of the order 10^{-14} near the surface. So if I want to know why this abundance is so low it is important to know if these species are formed by H or H_2 addition.

2.2.5 Temperature determination

ProDiMo uses the thermal balance to determine the temperature, assuming that the net gain of the thermal energy is equal to zero. The heating and cooling rates do not only depend on the kinetic gas temperature but also on the particle densities of the chemical species. However the particle densities also depend on the kinetic gas temperature. To solve this ProDiMo uses an iterative process during which the kinetic gas temperature is varied and the chemistry resolved so many times until the system converges (Woitke, P., Kamp, I., and Thi, W.-F., 2009).

2.3 Model used by Agúndez et al.

The model used by Agúndez et al. (2008) uses a similar structure.From their parper The gas density decreases radially as a power law, for this the formulas are very similar to those that are introduced in paragraph 2.2.2 (Agúndez et al., 2008). The region that is focused on is the part above the disk midplane between a radius of 1 and 3 AU, here the gas temperature ranges between 300 and 3000 kelvin.

2.3.1 Parameters in the Agúndez et al. model

The parameters used for the the 2018 model were given in table one of Agúndez et al. (2018), the parameters used in Agúndez et al. (2008) were collected from the text.

Parameters 2018	Value
Disk	
Disk mass	0.01 $M_\odot$
Inner disk radius	0.5 AU
Outer disk radius	500 AU
Gas-to-dust mass ratio	100
Radial surface density power index	1.0
Dust composition	70 % silicates
	30 % graphites
Minimum dust grain radius	0.001 μm
Maximum dust grain radius	1 μm
Dust size distribution power index	3.5
Cosmic-ray ionization rate of H_2	$5 \times 10^{-17}\,\mathrm{s}^{-1}$
TTauri star	
Stellar mass	0.5 $M_\odot$
Stellar radius	2 $R_\odot$
Stellar effective temperature	4000 K

TABLE 2.3: Parameters used by Agúndez et al. table 1 of Agúndez et al., 2018

Parameters 2008	Value
Disk	
Inner disk radius	0.1 AU
Outer disk radius	> 50 AU
Maximum dust grain radius	0.25 μm
Cosmic-ray ionization rate of H_2	1.2×10^{-14} s^{-1}
TTauri star	
Stellar mass	0.7 $M_\odot$
Stellar radius	2.6 $R_\odot$
Stellar effective temperature	4000 K

TABLE 2.4: Parameters used by Agúndez et al. this table is constructed from the values found in Agúndez et al., 2008

2.3.2 Chemistry

The model used by Agúndez et al. (2008) included 76 species, of which 29 neutral species, 5 negative ions, free electrons, 41 positive ions and no ices. In this model, reactions such as neutral-neutral, ion molecule bimoleculair reactions, three body processes, thermal dissociation and reactions induced by X-rays are included(Agúndez et al., 2008). In order to understand the chemical routes towards the simple molecules a few time dependent chemical models were used. This model uses the chemical code and network from Cernicharo (2004). The chemical network and rates are checked against the NIST (J. A. Manion and Frizzell, 2018) and UMIST (Le Teuff, Millar, and Markwick, 2000) database for astrochemistry. For the reaction rate coefficients for neutral-neutral reactions they use the same formula ProDiMo uses.
The new model used by Agúndez et al. (2018) includes 252 species of which 97 neutral species, 133 positive ions plus the negative ion H^-, free electrons and 20 ice molecules. In this model Agúndez et al. uses multiple databases for the reactions, these inlcude the UMIST2006(Woodall, J. et al., 2007) and UMIST2012 (McElroy, D. et al., 2013) databases which are used in ProDiMo. They calculate their initial abundance using a pseudo time dependent chemical model (where chemical evolution is solved under fixed physical conditions) of a cold dense cloud with standard the parameters, hydrogen density of 2 x 10^4 cm^{-3}, temperature of 10 K, cosmic ray ionization of 5 x 10^{-17} s^{-1} and a visual extinction of 10 mag at a time of 0.1 Myr. The model runs for a million year and gives the output (Agúndez et al., 2018). In contrary to the model of the 2008 the new model does not include X-rays.

In figure 2.3 the main synthetic path for the creation of C_2H_2, CH_4 and HCN are displayed according to Agúndez et al. (2008). The thickness of the arrow indicates the activation energy. This figure shows that the path towards these simple molecules is through reactions with H_2.

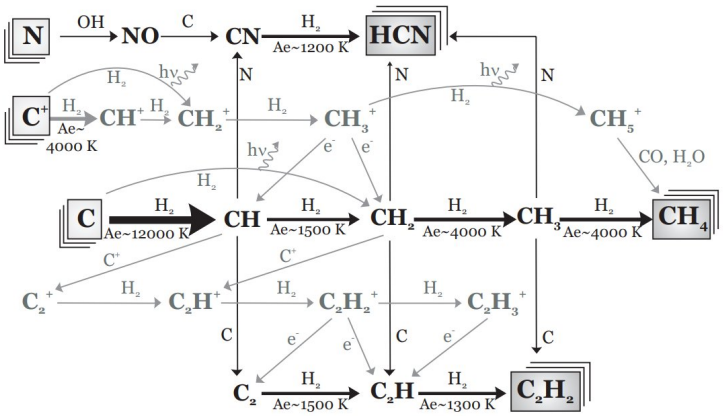

FIGURE 2.3: Main synthetic routes for the formation of C_2H_2, CH_4 and HCN used by Agúndez, Figure 2 from Agúndez et al. (2008)

2.3.3 Temperature determination

In the 2018 model by Agúndez et al. they assume that in the upper regions where $A_V < 0.01$ the temperature equals the evaporation temperature. They calculate the evaporation temperature as the temperature at which the most probable speed of the particles equals the escape velocity. For $1 < A_V < 0.01$ the gas temperature is approximated trough a linear interpolation with the height in the disk. For $A_V > 1$ the gas is assumed to be thermally coupled with the dust such that $T_{gas} = T_{dust}$.

Chapter 3

Results

3.1 Difference in species

The ProDiMo model (Woitke, P., Kamp, I., and Thi, W.-F., 2009) has a lot more different species than the model used by (Agúndez et al., 2008). ProDiMo uses 235 species while the model used by Agúndez et al. has only 76. However there are some molecules used by Agúndez et al. that do not exist within the ProDiMo model. These species are C^-, O^-, OH^-, HOC^+, CN^-, N_2H^+, H_2NC^+ and CNC^+. Adding C^-, O^-, OH^- and CN^- to the model does not produce a significant change in relative abundance to make a visual difference in the plots.

The model used by Agúndez et al. (2018), has 252 speciesof which 97 are neutral species, 133 positive ions plus the negative ion H^- and free electrons and 20 ice molecules. Comparing this with ProDiMo which has 69 neutral species, 100 positive ions plus the negative ions H^-, PAH^- and free electrons and 63 ice molecules. We see that Agúndez has more neutral species and ions inside his model. By comparing the different species we see that Agúndez et al. (2018) use a lot more carbons chains op to $C_{10}H_3$, while ProDiMo only goes up to C_3H_3. These large carbon chains do not appear to be part of the inner 3 AU, so this difference should not have an impact on that area. ProDiMo does have a lot more ice species.

3.1.1 Running ProDiMo with 0 instead of 63 ice molecules

Running ProDiMo with no ices decreases the relative abundance of C_2H_2, CH_4 and HCN. These species now only exist within a radius smaller then 0.5 AU in the midplane. This run did not give a result that would be useful for the problem of the difference in abundance.

3.1.2 Running ProDiMo with 18 instead of 63 ice molecules

By removing all ices from ProDiMo that Agúndez does not use we see that the C_2H_2 ice in the midplane at a radius of 3 AU grows larger in abundance. In the upper layers of the disk there is not a noticeable difference. The ices C_2H_6 and $HCOOH$ are part of the Agúndez et al. model but these do not exist in ProDiMo. C_2H_6 and $HCOOH$ do not not exist within ProDiMo so adding these as ice, does not have any influence. This is why the run is with 18 ice molecules instead of the 20 used by Agúndez et al. (2018).

CH_4	C_2H_2	C_2H_4	H_2O	O_2	CO	CO_2	H_2CO	CH_3OH
NH_3	N_2	HCN	H_2S	CS	H_2CS	SO	SO_2	OCS

TABLE 3.1: Ices left in the model

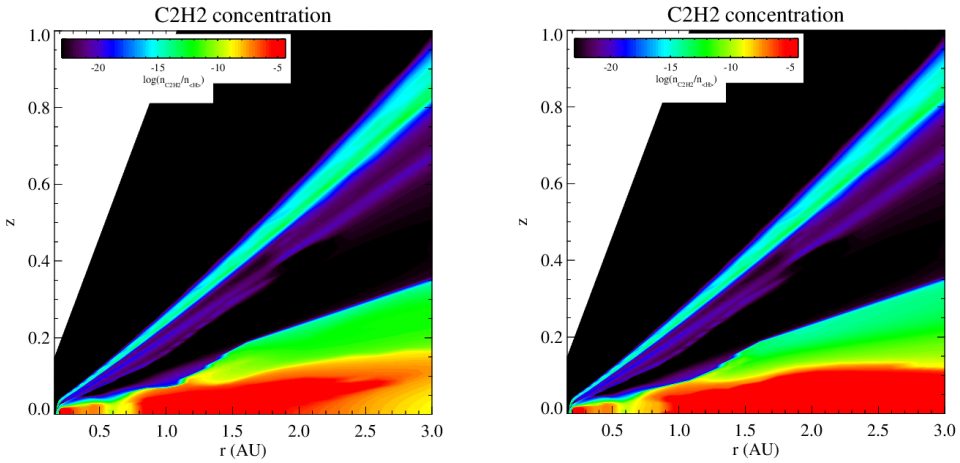

(A) 63 ices (B) 18 ices

FIGURE 3.1: Result of removing most of the ices and only including the 18 shown in table 3.1

As another test it is interesting to know what happens when C_2H_2 ice is removed from the model. By removing C_2H_2 ice, the main destruction and formation reactions in the midplane become the same as those in the surface layers. Despite losing the main destruction reaction it does not change the relative abundance of 10^{-5} in the midplane compared to the original run. The model of Agúndez et al. (2008) did not use any ices, since the focus for this model was the upper region in the disk. That model still had a high relative abundance in the surface. Hence the solution to the difference between ProDiMo and Agúndez et al. should not be in the ices.

3.2 Reactions

By comparing the reactions in ProDiMo with the reactions in the chemical ratefile provided by Marcelino Agúndez, it became quite clear that the ratefile provided by Marcelino Agúndez had a lot more three body reactions. However this should not have any impact on the abundance because almost all of the three body reactions involve carbon species with 4 or more carbon atoms, which do not play a role in the inner 3 AU. By comparing the reactions almost all of the core reactions for the creation and destruction for C_2H_2, HCN, and CH_4 were there along with the path towards them. ProDiMo does have an additional destruction reaction $C_2H_2 + H$ –> C_2H_3. By using one of the packages of ProDiMo (Woitke, P., Kamp, I., and Thi, W.-F., 2009) called chemanalyse we can see which reactions are dominant in certain areas. In the midplane the dominant reactions are all trough ices. Using this package I had hoped to find the creation pathway from which C_2H_2 originates in the surface layers. After removing both of the dominant creation reactions, where C_2H_2 originates from C_2H_3 and C_2H_2 ice, there is no longer a single reaction that dominates in creating the C_2H_2 abundance, this makes it hard to determine the main creation reaction. By using this package on C_2H_2 we get the following relative abundance plot shown on the left in figure 3.2.

The black area between the green and blue area in figure 3.2 there is a relative abundance smaller than 10^{-22} for C_2H_2,while this is part of the area in which Agúndez et al. (2018) has an abundance of 10^{-5}. By checking this area, the main formation

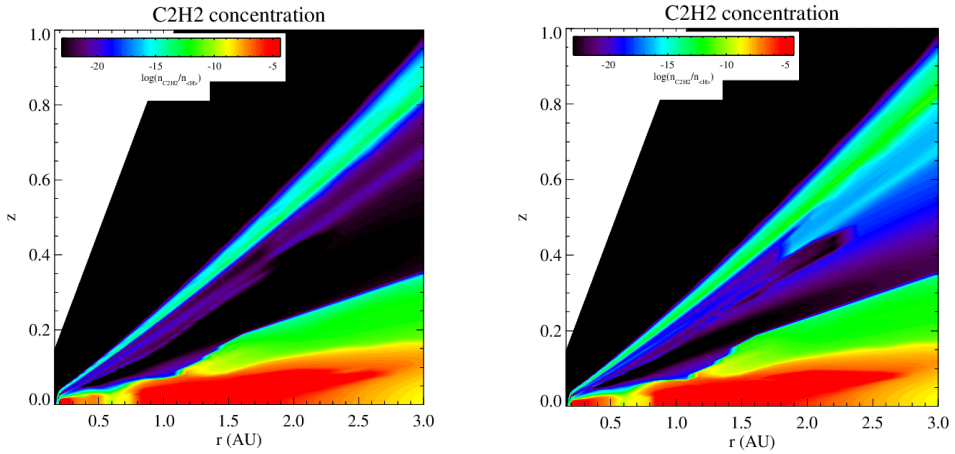

FIGURE 3.2: The left figure shows relative abundance of C_2H_2 with no changes to the model, the right figure shows the relative abundance of C_2H_2 after removing the main and secondary destruction reaction for C_2H_2 from the upper region from the model

reaction is found to be C_2H_3 + H –> C_2H_2 + H_2 and the main destruction reaction is C_2H_2 + H –> C_2H_3. From these reactions "C_2H_2 + H –> C_2H_3" does not exist within the UMIST2012 database nor in the reaction rate file provide by Agúndezet al. This reaction was added to ProDiMo and originates from a book called combustion chemistry written in 1984. The rate constants can be found within the NIST Chemical kinetics database (J. A. Manion and Frizzell, 2018).

Removing this reaction changes the abundance with a factor 10, which is not visible. The reaction C_2H_2 + H –> C_2H_3 is the main destruction and the secondary destruction reaction is by photo dissociation. If I remove both of these processes the abundance is shown on the right side in figure 3.2. So removing the main and secondary destruction channel does have some impact. The relative abundance of C_2H_2 went up to 10^{-16}, but this is still too low compared to a relative abundance of 10^{-5}.

3.3 Hydrogen abundance

The hydrogen abundance is of quite importance because part of the issue is that in Agúndez et al. (2008) the main creation channel is trough H_2 addition, which is not visible within the ProDiMo model. So inspecting where the H to H_2 transition lies with respect to where C_2H_2 is abundant both models might be helpful to understand why ProDiMo and Agúndez et al. (2008) have different relative abundances C_2H_2.

The abundance for H and H_2 is shown in figure 3.3. In the abundance for H_2 there is a weird bump around a radius of 2 AU. If we compare this with the abundance shown in figure 1.1, in the Agúndez at al. model there is a high C_2H_2, HCN, and CH_4 abundance of 10^{-6} close to the surface. In this area the relative abundance in ProDiMo is between 10^{-8} and 10^{-10}. If the main pathway for C_2H_2, HCN, and CH_4 is through H_2 addition as Agúndez at al. showed with figure 2.3, this would imply that in the model of Agúndez et al. (2008) there exist H_2 in large relative abundances closer to the disk surface than in ProDiMo.

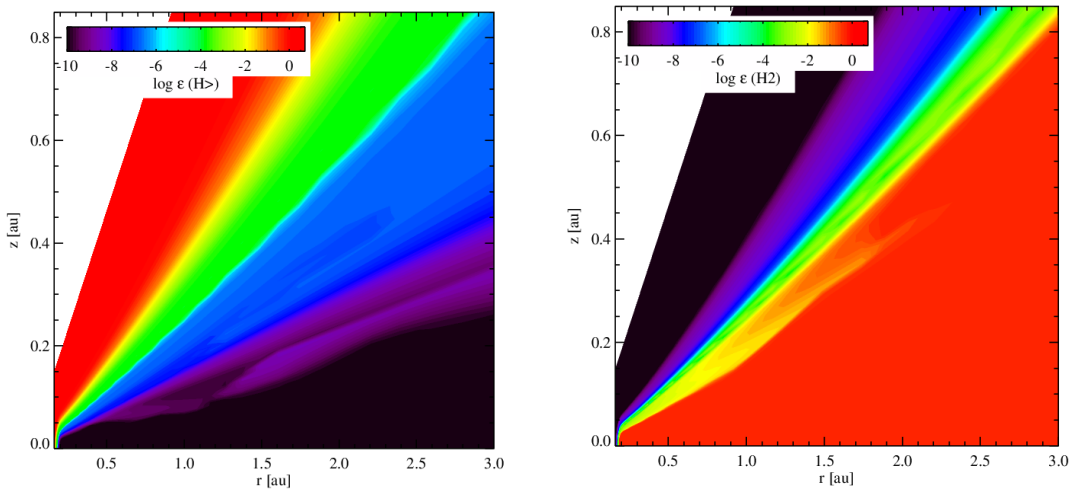

(A) H (B) H2

FIGURE 3.3: Abundance of H and H_2, shown agianst the radius and height of the disk

3.4 Reaction rate coefficients

The paper of Agúndez et al. (2008) referenced to a paper written by Cernicharo (2004) for the rate coefficients. This paper supplied for 31 of the main reactions the rate coefficients. This table is shown in appendix A. Besides two reactions all reactions that both models had in common, had rate coefficients that were within a factor 5 of each other. The two rates that did not match were actually a mistake from my side but it gave an interesting result. These two reactions were $H_2 + C_2H$ –> $C_2H_2 + H$ and $H_2 + N$ –> $NH + H$. The rate coefficients are shown in figure 3.4. All other rate coefficient comparison plots of reactions in common between Prodimo and Agúndez et al. are shown in Appendix A.

3.4.1 Wrong reaction rate coefficient, with an interesting result

For the reaction $C_2H + C_mH_2$ –> $C_mH + C_2H_2$ there is clear difference in the reaction rate coefficients (figure 3.4A). The reaction rate coefficient used by Cernicharo (2004) is a constant, while the reaction rate coefficient used in ProDiMo increases as the temperature increases. A possible cause for why the relative abundance of C_2H_2, CH_4 and HCN is less than what Agúndez et al. (2008) got is that reactions in ProDiMo have lower rate coefficients. For example for the creation of C_2H_2 there are at least four reactions needed according to figure 2.3. If chemistry was nicely linear and all four of these rate coefficients are a factor ten lower the entire formation would be a factor thousand lower.

The difference in abundance can be seen in figure 3.5; the abundance change for CH_4 and HCN can be found within appendix C. This is the result of changing the values for the rate coefficient in ProDiMo to the mistakenly identified value of Cernicharo (2004). This increase in relative abundance in the upper regions of the disk seems to be close to what we are looking for. However after taking a closer look at the reaction scheme shown in appendix A, we determined that m and n cannot be zero. If m and n can be zero this would mean that reaction 19 and 27 are exactly the same while their A component varies with a factor 1000. Which means the compared

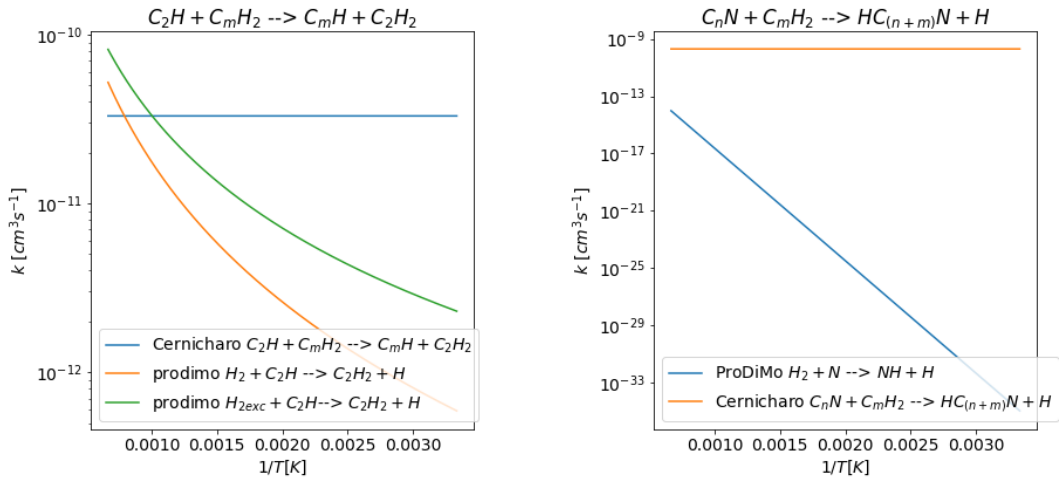

(A) (B)

FIGURE 3.4: Rate coefficients of two reactions for which was assumed that n and m could be equal to zero

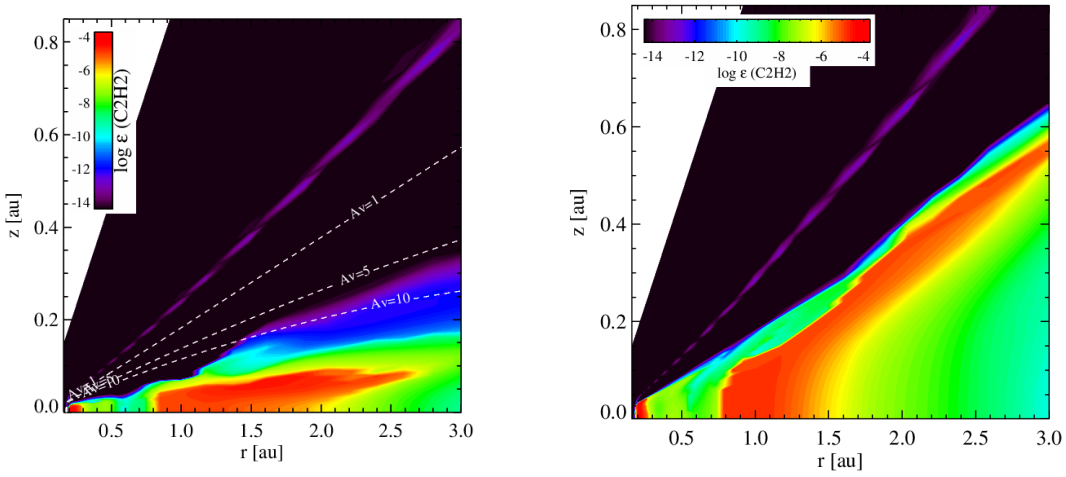

(A) Before (B) After

FIGURE 3.5: Difference in relative abundance due to changing the rate coefficients of $H_2 + C_2H$ –> $C_2H_2 + H$ and $H_2 + N$ –> $NH + H$

reactions in figure 3.4 are not the same. However despite this rate coefficient being wrong the high abundance of C_2H_2,CH_4 and HCN did shift towards the disk surface. The formation reactions with H_2 addition are not dominant near the disk surface in the ProDiMo model. However these are the reactions Agúndez et al. (2008) uses the get the high abundance near the disk surface.

3.4.2 Rate comparison between ProDiMo and Agúndez et al.(2018)

Marcelino Agúndez shared the reaction rate file that was used for the newer model with me. Using this file all of the reactions for the main synthetic path in figure 2.3 were compared with the reactions used in ProDiMo. This was done by plotting the

rate coefficient against the inverse temperature. From this it became clear that in the new model all compared reactions are within a factor ten of each other. There are a few exceptions where the difference is larger than a factor ten; however for those cases the rate coefficient is below 10^{-16} so this difference should not have any significant influence. All compared reactions that are not exactly the same or constant are shown in appendix B. From this it is save to say that the rate coefficients are not responsible for the problem of different abundances. Giving these findings, the solution of the initial problem of abundance difference has to be searched for in the physical disk structure.

3.4.3 Additional changes to the model that gave no results

There was also a run in which the a rate coefficient of all C_nH_n + H_2 reactions up to C_2H_2 were increased with a factor of 100 in order force ProDiMo to go into the H_2 addition channel in the surface layers. However this did not have any significant impact, which indicates that having a large amount of C_2H_2 cannot exist in steady stat near the surface in the current ProDiMo.

Furthermore because Agúndez et al. (2008) was based on the UMIST2006 database, there was also a ProDiMo model run with the UMIST2006 database instead of the UMIST2012 version, but this did not have any impact on the relative abundance.

3.5 Fundamental differences between the models

Between ProDiMo and the model use by Agúndez et al. (2018) there are also some fundamental difference, 3 large differences are the way in which the temperature is defined, the time the models runs, and that the model used by Ag'undez et al. has no X-rays. In the coming sections I will explain the difference between the temperature determination and timescale.

3.5.1 Temperature

From Agúndez et al. (2018), it is clear that there is difference in the way his model determines the temperature. In the ProDiMo model the gas temperature is calculated from a heating/cooling balance, while in the model of Agúndez et al. the gas temperature is split up in three different sections. Below $A_v = 1$, the gas temperature is assumed to be equal to the dust temperature . In an article written by Woods and Willacy (2007), they state that the gas temperature can be underestimated by 2 orders of magnitude if it is assumed to be the dust temperature throughout the disk, this is something that is meant for the entire disk so using $T_{gas} = T_{dut}$ only for the midplane is valid approximation.

3.5.2 Timescales

Another difference between the model is the time used for the chemical evolution to reach the calculated abundances, in other words the age of the disk. ProDiMo forces the model to go to full steady state, while the model by Agúndez et al. (2018) only runs for a million years. In the ProDiMo model the ices have developed a lot more than in the model by Agúndez et al. In ProDiMo for almost all species the main destruction and main creation channel in the midplane is caused by the phase change to ice.

3.6 Reproducing the Agúndez et al. model with ProDiMo, by means of changing the disk parameters

In all of the previous runs discussed in section 3.2 there were only changes to the species or rates, all the disk parameters were kept the same. By comparing table 2.1 with table 2.3, it shows that a lot of disk and stellar parameters are different. So the next test was to run the ProDiMo model with the parameters from the model by Agúndez et al. (2018). ProDiMo uses the stellar luminosity to calculate the parameter for the radius. The original model had a stellar radius of 2.25 $R_\odot$, So using the Stefan-Boltzmann relation for a blackbody with a radius of 2.0 $R_\odot$, the new luminosity was calculated to be 0.79 $M_\odot$. All other parameters could be directly changed in the model.

The disk Parameters that have been changed in ProDiMo

Parameter	Old value	New value
Disk mass	0.015 $M_\odot$	0.01 $M_\odot$
Inner disk radius	0.16 AU	0.5 AU
Outer disk radius	100 AU	500 AU
Dust composition	50 % silicates	70 % silicates
	50 % graphites	30 % graphites
Minimum dust grain radius	0.005 μm	0.001 μm
Maximum dust grain radius	750 μm	1 μm
Dust size distribution power index	3.0	3.5
Cosmic-ray ionization rate of H_2	$1.7 \times 10^{-17}\,\mathrm{s}^{-1}$	$5 \times 10^{-17}\,\mathrm{s}^{-1}$
Stellar mass	0.7 $M_\odot$	0.5 $M_\odot$
Stellar radius	2.25 $R_\odot$	2 $R_\odot$
Stellar effective temperature	4000 K	4000 K
Luminosity	1 $L_\odot$	0.79 $L_\odot$

The most important parameter change is the maximum dust grain radius, this value changes by a factor of 750, while all other changes only differ by a maximum factor of five. The result for C_2H_2 from changing these parameters is shown in figure 3.6. In the right panel of this figure the abundance for C_2H_2 is no longer concentrated towards the midplane and reaches a value of 10^{-5} in a disk surface layer. The results for CH_4 and HCN can be found in appendix C.2. There are still some differences within the midplane but this is due to that the midplane of Agúndez et al. is colder. This causes the transition from water vapor to ice to be at a different radius. In the model by Agúndez et al. the entire midplane is frozen, while in ProDiMo the water starts to freeze out at a radius of 1 AU. In figure 3.6 the radial extinction of one, five and ten is plotted with a dashed line. In the model where the parameters are changed the extinction increases faster with respect to the depth in the disk. This is because the of the decreased maximum dust grain radius.

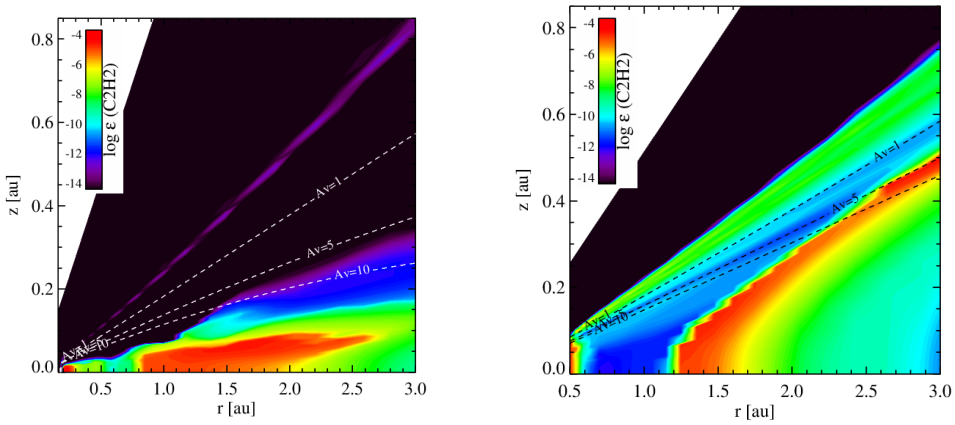

(A) ProDiMo old (B) ProDiMo new

FIGURE 3.6: The relative abundance of C_2H_2 produced by ProDiMo after changing the parameters, the dashed lines indicates where the radial extinction is equal to one, five and ten

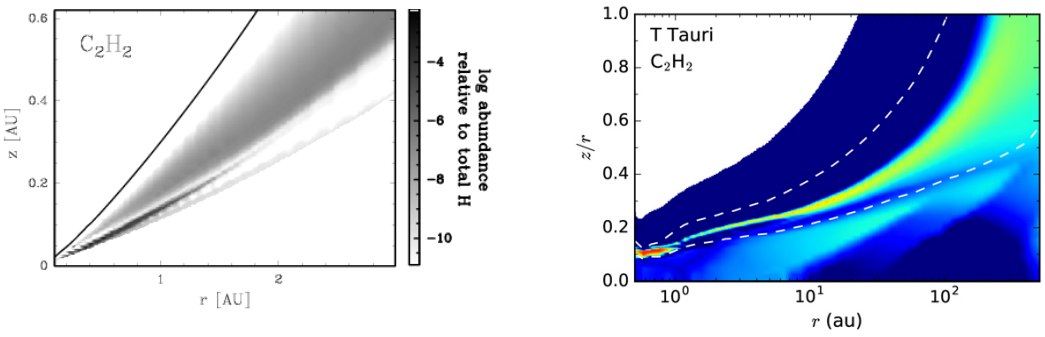

(A) Agúndez et al. (2008) (B) Agúndez et al. (2018)

FIGURE 3.7: figure A is taken from Agúndez et al. (2008) an figure B is taken from figure 6 of Agúndez et al. (2018), on the left is the relative abundance for C_2H_2 for the inner 3 AU, and on the right there is the relative abundance for C_2H_2 for the whole disk

3.7 Vertical cut

By making a vertical cut of the data it is easier to see if what happens exactly to species within the disk. This vertical cut is constructed by plotting the relative abundance against the column density. So the lowest density is the disk surface and the densest part is the midplane. Marcelino Agúndez shared some of his data from his 2018 model with us. From this data it was possible to construct a vertical cut.

3.7.1 Difference between the original ProDiMo and remade ProDiMo model

By comparing the vertical cut of the new and old model we see that the H/H_2 transition has moved from a column density of 24 cm^{-2} to 20 cm^{-2} in figure 3.8. The H/H_2 transition has moved because the maximum grain size from decreased from 750 μm to1 μm. The mass of the combined dust is constant, so if the particles are smaller this

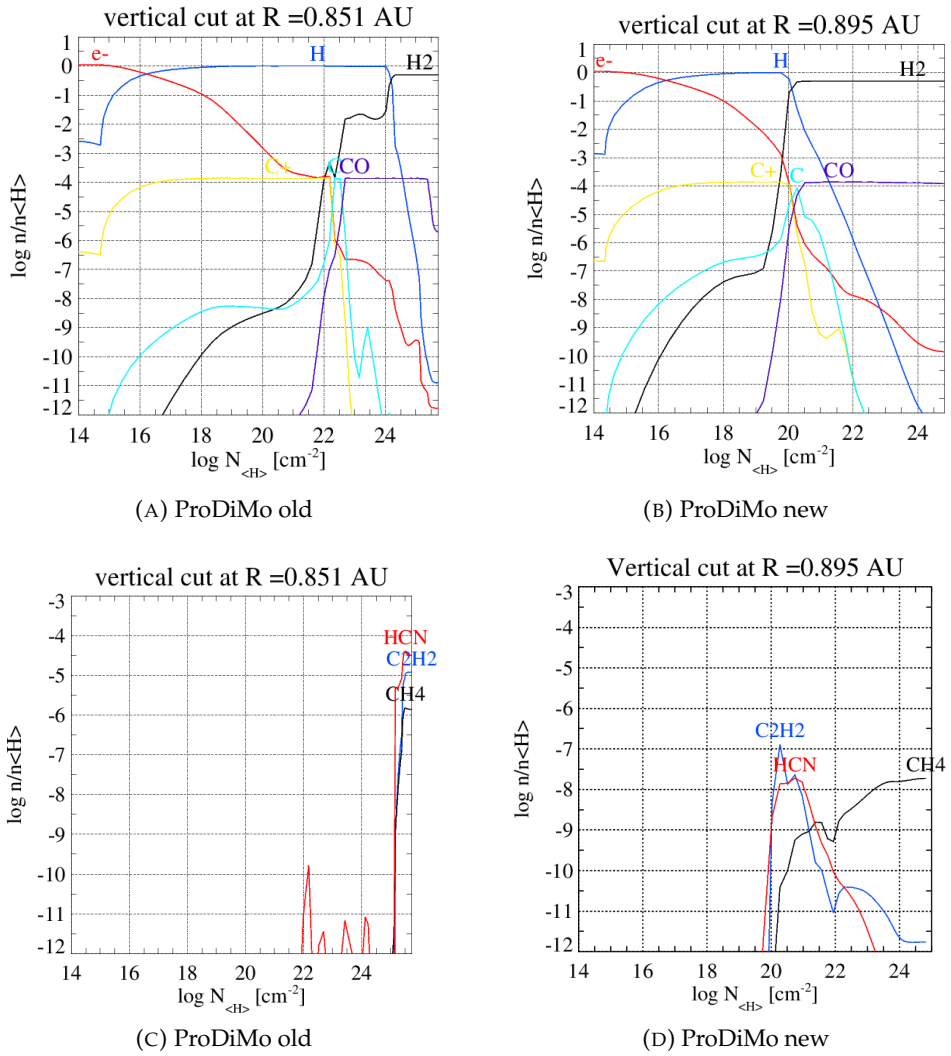

(A) ProDiMo old

(B) ProDiMo new

(C) ProDiMo old

(D) ProDiMo new

FIGURE 3.8: Vertical cut for the species H, H_2, e^-, C, C^+, CO and C_2H_2, CH_4, HCN with the old disk parameters vs the new disk parameters

means there are in total more dust particles, resulting in a larger effective area. This leads to a more opaque disk which affects the extinction in the disk. So the disk is more opaque which means photons penetrate less into the disk. Because of this the photo-dissociation region for H_2 lies a lot higher with respect to the midplane in the disk than in the original model.

For C_2H_2, CH_4 and HCN there is a large increase in relative abundance for a column density of 20 cm^{-2} shown in figure 3.8. In the model with the original values all species are completely on the right at the highest column density, which is the disk midplane. In the model with changed parameters the species are more centered with respect to the height of the disk.

3.7.2 Difference between ProDiMo and Agúndez

Using the data Marcelino Agúndez shared with us it was possible to construct a vertical cut showing the relative abundance as a function of column density at a certain radius. For a radius of 0.878755, 0.763209, 0.662856 and 1.544422 AU, a vertical cut

was made. The reason these numbers are not exact is because in the data received from Marcelino Agúndez. the values were given with a certain stepsize. Which resulted in these radii. ProDiMo uses a certain stepsize so it is not possible to create a cut at a specific radius. From ProDiMo I took the values that were closest to the given radii from the received data. Between 0.5 and 1 AU is the interesting part, because this is the part where the Agúndez et al. (2018) model has the high abundance of 10^{-5}, as shown in figure 1.2. At a radius of 1.5 AU, ProDiMo has the high C_2H_2 abundance of 10^{-5} in the surface as shown in figure 3.6B.

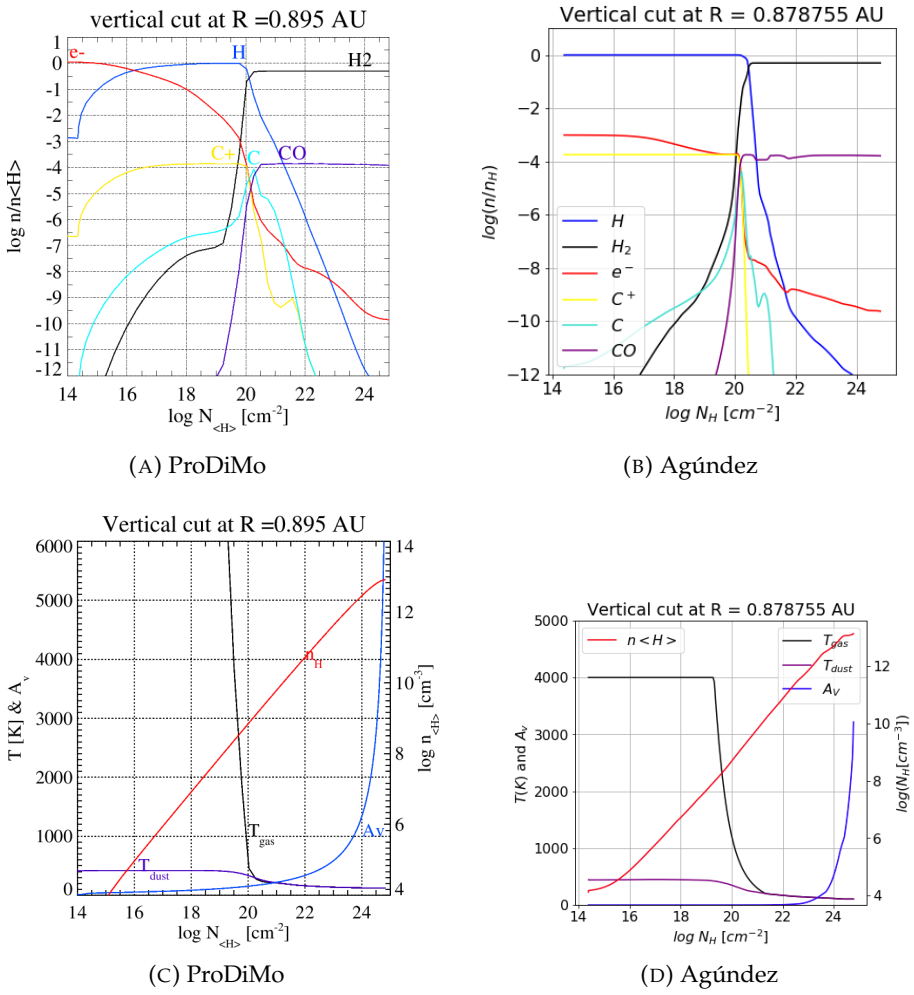

(A) ProDiMo (B) Agúndez

(C) ProDiMo (D) Agúndez

FIGURE 3.9: Vertical cut showing the most basic species and a vertical cut showing T_{gas}. T_{dust}, A_v and n_H as a function of column density in the disk at R around 0.89

From this vertical cut the H/H_2 transition seems to be at the same column density of 20.5 cm^{-2}. A visible difference between figure 3.9 A & B is that in ProDiMo H and C^+ decrease in abundance towards the surface. This decrease is due to the ionization to H^+ and C^{++}; this ionization is not visible within the vertical cut for the Agúndez et al. model. For C^+ this is because the Agúndez et al. model does not have double ionized species. Furthermore the Agúndez et al. (2018) model does not include X-rays. Because of this there are no high enough energized photons to ionize hydrogen. The old model (Agúndez et al., 2008) did include X-rays, however

there is no data to construct a vertical cut for the old model.

By constructing a vertical cut of T_{gas}, T_{dust}, A_v and n_H we see some of the disk structure that is different. The biggest difference is that in the model of Agúndez et al. the gas temperature is capped at 4000 Kelvin. ProDiMo has a temperature of almost 25000 Kelvin in the surface. This is likely due to X-ray heating. What is also interesting to see in the vertical cut made from the Agúdez et al. data is that the location where $A_v = 1$ can be determined in the graph. This is the location where T_{gas} becomes equal to T_{dust}. Which is for both models around a column density of 21 cm^{-2}, this is also the location where Hydrogen gets ionized. By comparing this with figure 3.8D, we see that at a column density of 21 cm^{-2} the relative abundance of C_2H_2 and HCN peaks. From this it is save to say that the main creation pathway for the ProDiMo network for C_2H_2,CH_4 and HCN is trough H_2 addition. In terms of density and opacity the disks are similar, as can be seen in figure 3.9 C and D.

A lot more figures with vertical cut at different radii can be found in appendix D.

Chapter 4

Conclusion

The aim of this thesis was to find the difference between te models that caused a difference in the relative abundance for C_2H_2, CH_4 and HCN between ProDiMo and the model by Agúndez et al.

There are some differences in the chemistry but not one of these differences had enough impact to reproduce the result of Agúndez et al. shown in figure 1.1. Some of the species, especially the amount of ices are really different. Adding or removing species did not give the desired result. There was also the reaction $C_2H_2 + H$ –> C_2H_3 which did not exist within the model of Agúndez et al. and turned out to be one of the the main destruction mechanisms in ProDiMo. Removing it did not change the abundance. By comparing the reaction rate coefficients for the main synthetic path there were no significant differences between the models, all compared reaction rate coefficients had values very similar to each other.

The model used by Agúndez et al. only runs for a million years, this means the chemistry in the midplane has not reached steady state. Running the model for a million years is enough to reach steady state in the upper disk but not in the midplane. ProDiMo runs the model until it reaches steady state, so also the midplane has reached steady state in ProDiMo. This is also why ProDiMo has the main creation and destruction reactions in the midplane with ices.

Running ProDiMo with the same parameters that Agúndez et al. used for disk mass, disk radius, grain size, dust composition and cosmic ionization rate, resolved the problem of the difference in relative abundance. The results of this run shows the same values for the relative abundance of C_2H_2,CH_4 and HCN high up in the disk. The midplane is still different from the results Agúndez et al. showed us in figure 1.2. ProDiMo has relative abundances between 10^{-5} and 10^{-5} for the midplane and in the model by Agúndez et al. the relative abundance does not go higher than 10^{-10} for the midplane.

To conclude, the difference between the relative abundance has two main causes, which are the timescales and the grain size distribution. The grain size distribution has a large effect on the photo dissociation of H_2 which is one the the important reactants. Because the main pathway towards CH_4 and C_2H_2 is by H_2 addition. Thus by moving the location of the H/H_2 transition up in the disk, the relative abundance of C_2H_2,CH_4 and HCN also moved up in the disk with respect to the midplane. The temperature in Agúndez et al.'s midplane is lower then in ours because of the way they determined it causing their model not to be in steady state in the midplane.

For Future works it is interesting to run the model with a time dependent chemistry up to a million years to see what kind of effect this has on the midplane.

Appendix A

Compared rate coefficients with the 2008 model

The rate coefficients for the Agúndez et al. (2008) model are taken from table 1 from Cernicharo (2004). The values from Prodimo (Woitke, P., Kamp, I., and Thi, W.-F., 2009) are largely based on UMIST2012. This comparison of the two sets of rate coefficients focuses on the warm chemistry in the inner disk because that is were these reactions should occur.

MAIN REACTIONS INCLUDED IN THE MODEL

ID	Reaction	A ($cm^3\ s^{-1}$)	n	E (K)
R1	$C_nH + C_mH_2 = C_{n+m}H_2 + H$	2.7×10^{-10}	−0.43	0
R2	$C_2H + C_mH_2 = C_mH + C_2H_2$	3.3×10^{-11}	0.00	0
R3	$C_nH + C_mH = C_{n+m}H + H$	3.3×10^{-11}	0.00	0
R4	$C_nH + C_mH = C_nH_2 + C_m$	3.0×10^{-12}	0.00	0
R5	$C_2H + C_2H_4 = C_4H_4 + H$	2.0×10^{-11}	0.00	0
R6	$C + C_2H = C_3 + H$	3.3×10^{-10}	0.00	0
R7	$C + C_2H_2 = C_3H + H$	2.0×10^{-10}	0.00	0
R8	$C + C_2H_2 = C_3 + H_2$	2.0×10^{-10}	0.00	0
R9	$C + C_nH_m = C_{n+1}H_{m-1} + H$	3.3×10^{-10}	0.00	0
R10	$C_n + C_mH = C_{m+n} + H$	2.0×10^{-10}	0.00	0
R11	$H_2 + C = CH + H$	3.1×10^{-10}	0.16	11890
R12	$H_2 + C_2 = C_2H + H$	1.8×10^{-10}	0.00	1469
R13	$H_2 + C_n (n > 2) = C_nH + H$	1.0×10^{-14}	0.00	0
R14	$H_2 + C_nH = C_nH_2 + H\ (n > 2)$	4.2×10^{-12}	1.67	624
R15	$H_2 + CH = H + CH_2$	2.7×10^{-10}	0.00	1545
R16	$H_2 + CH_2 = H + CH_3$	5.2×10^{-11}	0.17	6400
R17	$H_2 + CH_3 = H + CH_4$	2.0×10^{-14}	2.84	3864
R18	$H_2 + CN = HCN + H$	1.6×10^{-12}	2.06	1334
R19	$H_2 + C_nN = HC_nN + H\ (n > 1)$	5.3×10^{-13}	0.00	0
R20	$H + CH = C + H_2$	1.3×10^{-10}	0.00	80
R21	$H + CH_2 = CH + H_2$	5.2×10^{-11}	0.00	−675
R22	$H + CH_3 = CH_2 + H_2$	1.0×10^{-10}	0.00	7600
R23	$H + CH_4 = CH_3 + H_2$	3.5×10^{-13}	3.11	3970
R24	$H + C_2H = C_2 + H_2$	8.4×10^{-11}	0.00	14330
R25	$CN + C_2H_4 = HCN + C_2H_3$	2.1×10^{-10}	0.00	0
R26	$CN + C_2H_4 = CH_2CHCN + H$	5.1×10^{-11}	−0.70	31
R27	$C_nN + C_mH_2 = HC_{n+m}N + H$	2.0×10^{-10}	0.00	0
R28	$O + CH_3 = H_2CO + H$	1.4×10^{-10}	0.00	0
R29	$O + C_2H_3 = OH + C_2H_2$	2.0×10^{-11}	0.00	0
R30	$CO + OH = CO_2 + H$	1.2×10^{-13}	0.95	−75
R31	$H_2 + OH = H_2O + H$	8.4×10^{-13}	0.00	1040

NOTE.—For this table, $k = A(T/300)^n e^{-(E/T)}$ and $T_k > 300$ K.

FIGURE A.1: Rrate coefficients from table 1 of Cernicharo (2004)

17 of these reactions are not plotted. These are reactions 12,16,20 and 22 because they have exactly the same values for the rate coefficients. Reactions 2,3,4,5,13,15,19,24,26 and 29 do not exist within ProDiMo. And reactions 6,9 and 10 are constant against temperature in both models and vary by less than a factor 2.

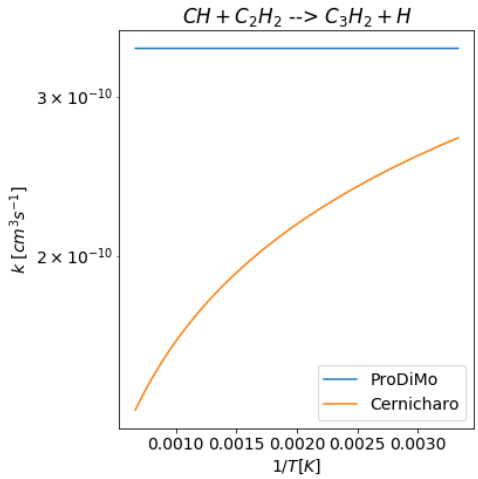

(A) Reaction 1

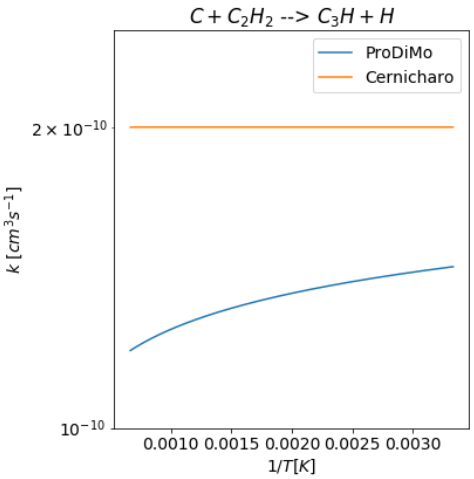

(B) Reaction 7

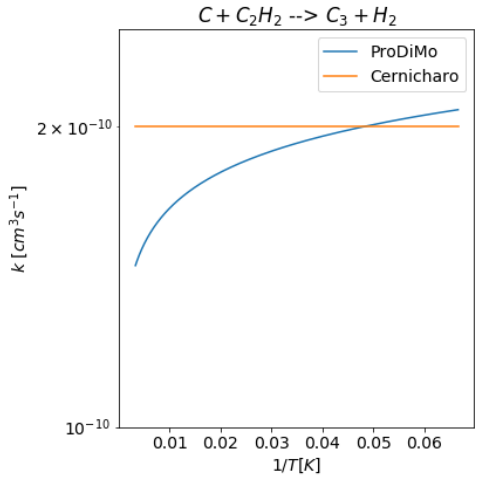

(C) Reaction 8

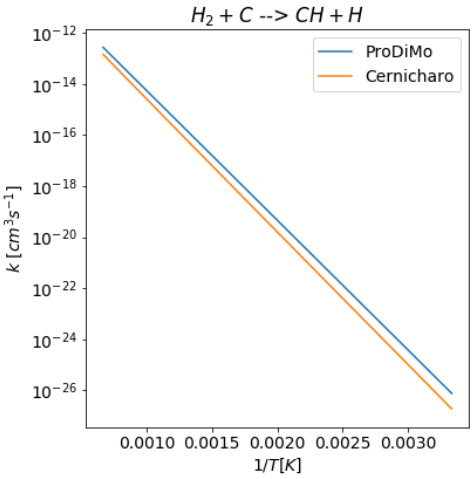

(D) Reaction 11

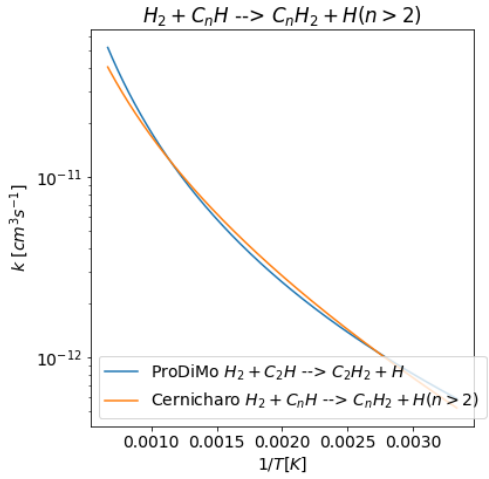

(E) Reaction 14

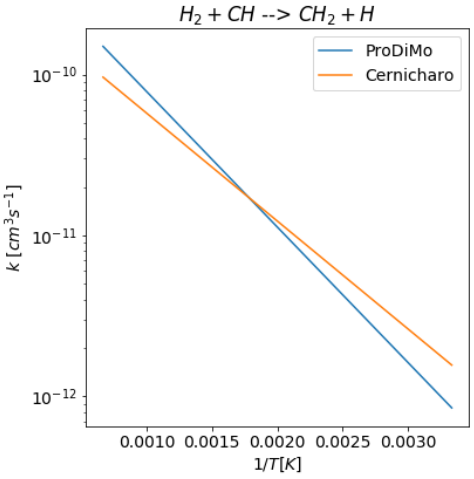

(F) Reaction 15

FIGURE A.2

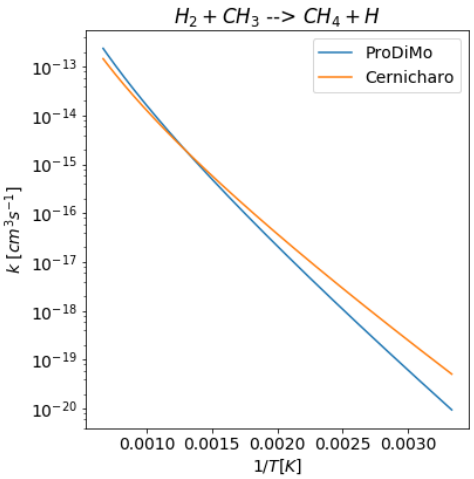

(A) Reaction 17

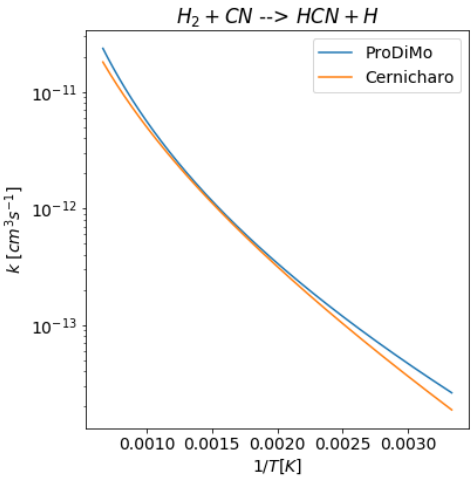

(B) Reaction 18

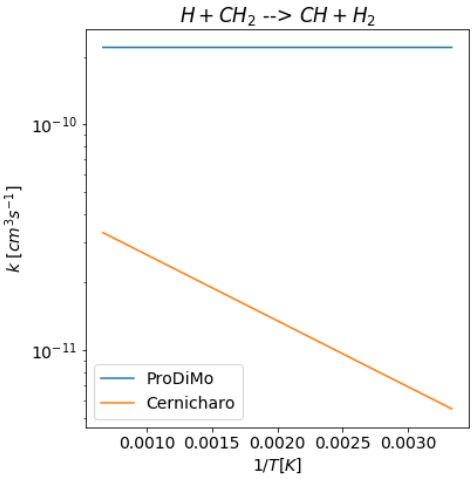

(C) Reaction 21

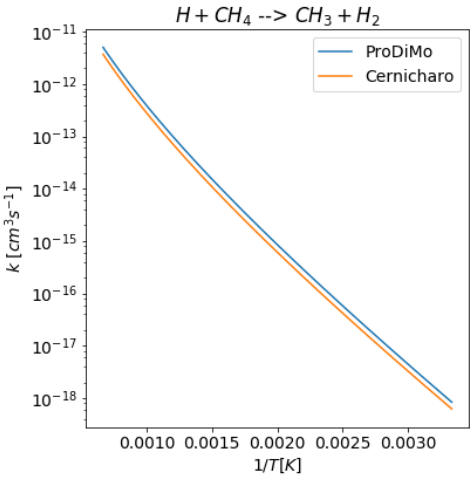

(D) Reaction 23

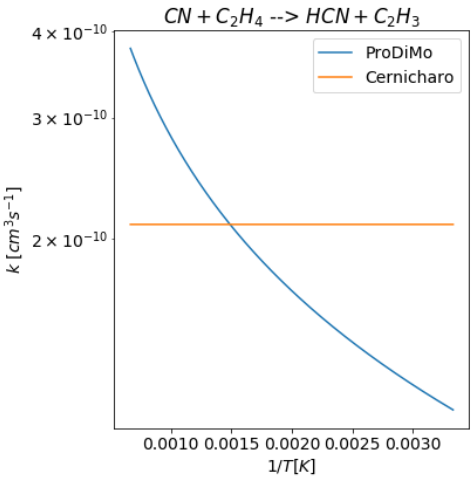

(E) Reaction 25

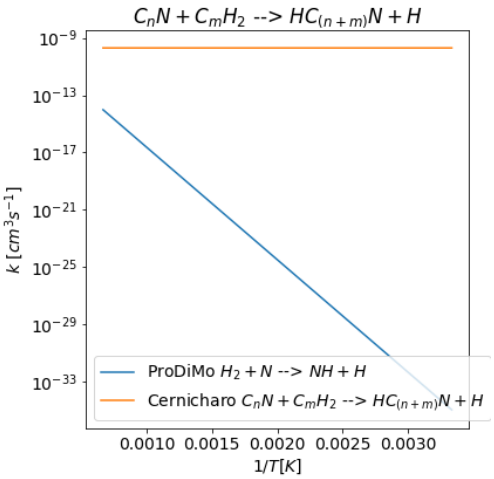

(F) Reaction 27

FIGURE A.3

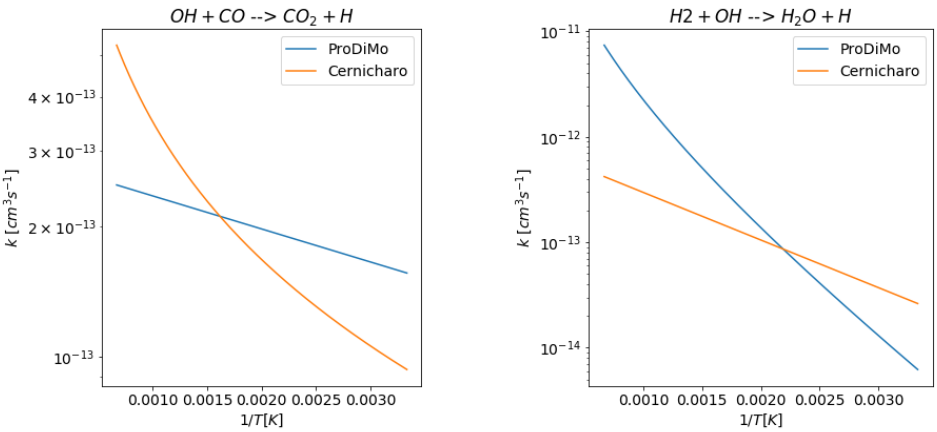

(A) Reaction 30 (B) Reaction 31

FIGURE A.4

Appendix B

Compared rate coefficients with the 2018 model

The rates for this comparison are taken from the reaction rate files we got from Marcelino Agundez. Besides the reaction $C_2H_2^+ + H_2 \rightarrow C_2H_3^+ + H$, all reactions from figure 2 of (Agúndez et al., 2008) have been compared. Rate coefficients that were exactly the same or both constants are not shown in the plots.

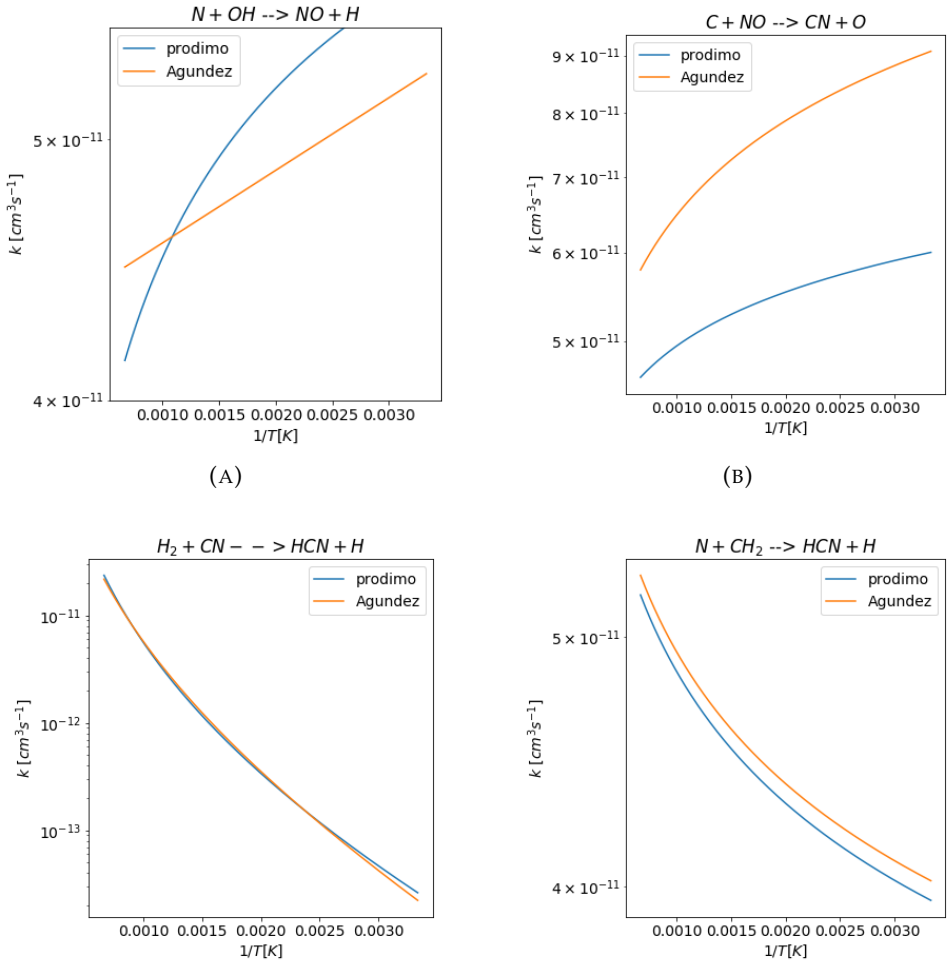

(A) (B)

(C) (D)

FIGURE B.1

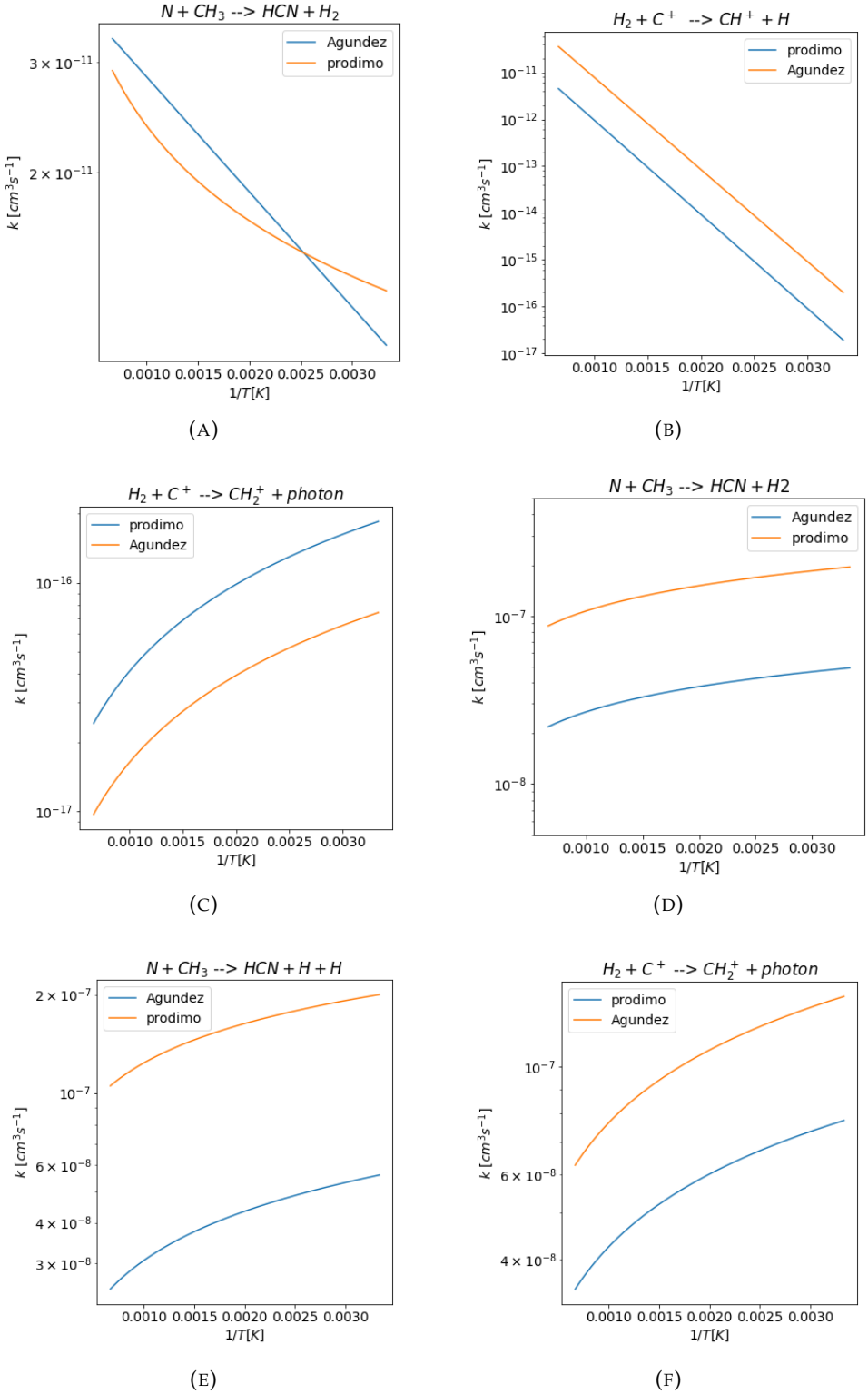
$N + CH_3$ --> $HCN + H_2$
Agundez
prodimo
3×10^{-11}
2×10^{-11}
$k\ [cm^3s^{-1}]$
0.0010 0.0015 0.0020 0.0025 0.0030
$1/T[K]$
(A)
$H_2 + C^+$ --> $CH^+ + H$
prodimo
Agundez
10^{-11}
10^{-12}
10^{-13}
10^{-14}
10^{-15}
10^{-16}
10^{-17}
$k\ [cm^3s^{-1}]$
0.0010 0.0015 0.0020 0.0025 0.0030
$1/T[K]$
(B)
$H_2 + C^+$ --> $CH_2^+ + photon$
prodimo
Agundez
10^{-16}
10^{-17}
$k\ [cm^3s^{-1}]$
0.0010 0.0015 0.0020 0.0025 0.0030
$1/T[K]$
(C)
$N + CH_3$ --> $HCN + H2$
Agundez
prodimo
10^{-7}
10^{-8}
$k\ [cm^3s^{-1}]$
0.0010 0.0015 0.0020 0.0025 0.0030
$1/T[K]$
(D)
$N + CH_3$ --> $HCN + H + H$
Agundez
prodimo
2×10^{-7}
10^{-7}
6×10^{-8}
4×10^{-8}
3×10^{-8}
$k\ [cm^3s^{-1}]$
0.0010 0.0015 0.0020 0.0025 0.0030
$1/T[K]$
(E)
$H_2 + C^+$ --> $CH_2^+ + photon$
prodimo
Agundez
10^{-7}
6×10^{-8}
4×10^{-8}
$k\ [cm^3s^{-1}]$
0.0010 0.0015 0.0020 0.0025 0.0030
$1/T[K]$
(F)

FIGURE B.2

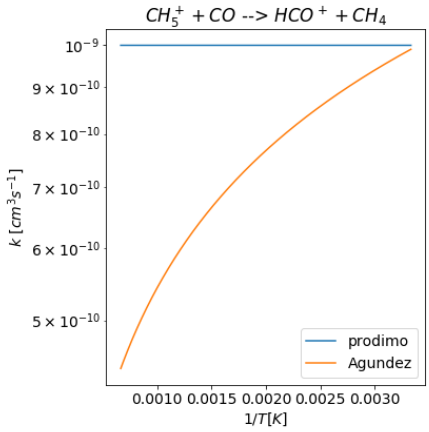

(A)

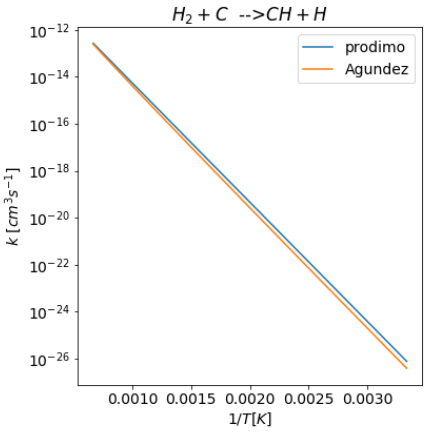

(B)

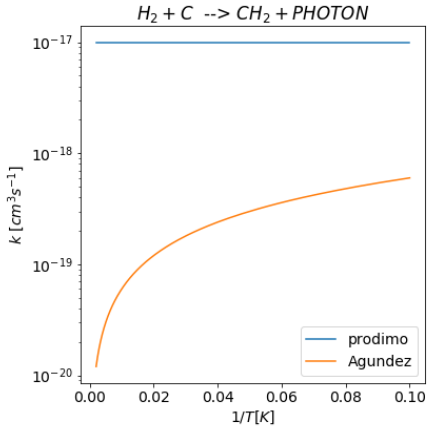

(C)

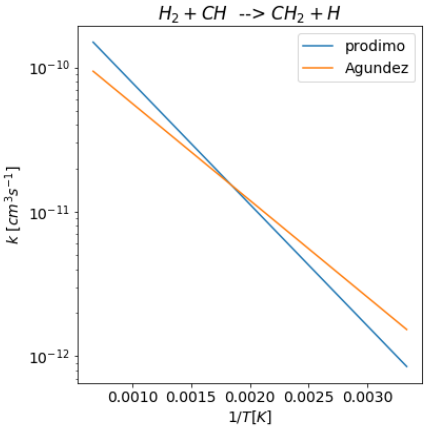

(D)

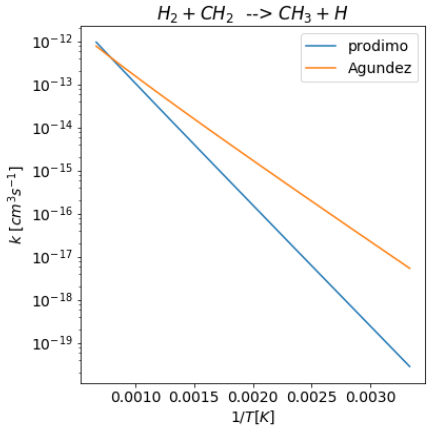

(E)

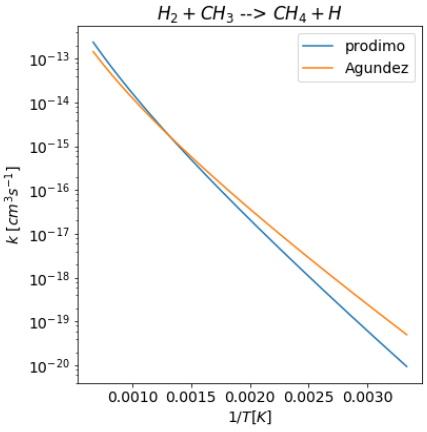

(F)

FIGURE B.3

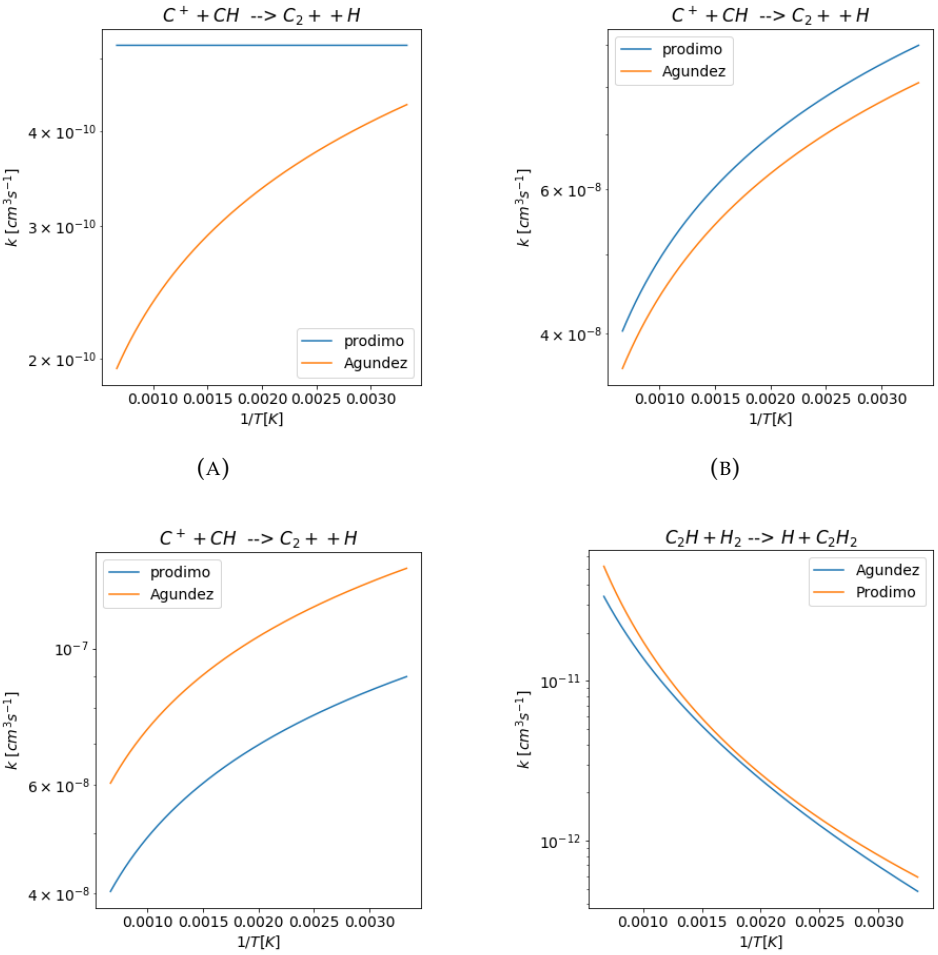

(A) (B)

(C) (D)

FIGURE B.4

Appendix C

Abundance for HCN and CH_4

C.1 Changing two reaction rate coefficients

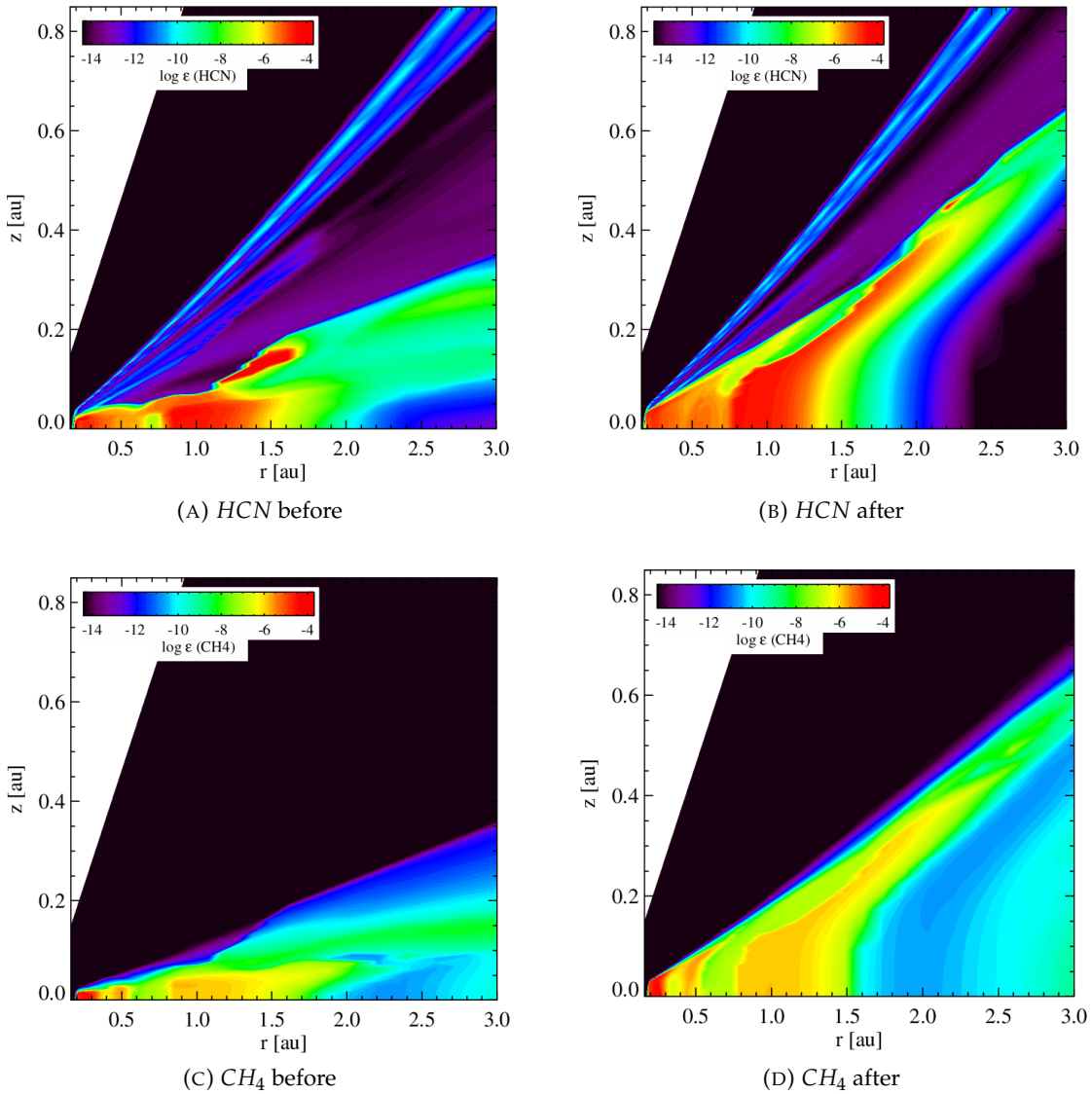

(A) HCN before

(B) HCN after

(C) CH_4 before

(D) CH_4 after

FIGURE C.1: Difference in relative abundance due to changing the rate coefficients of $H_2 + C_2H$ –> $C_2H_2 + H$ and $H_2 + N$ –> $NH + H$

C.2 Changing the parameters

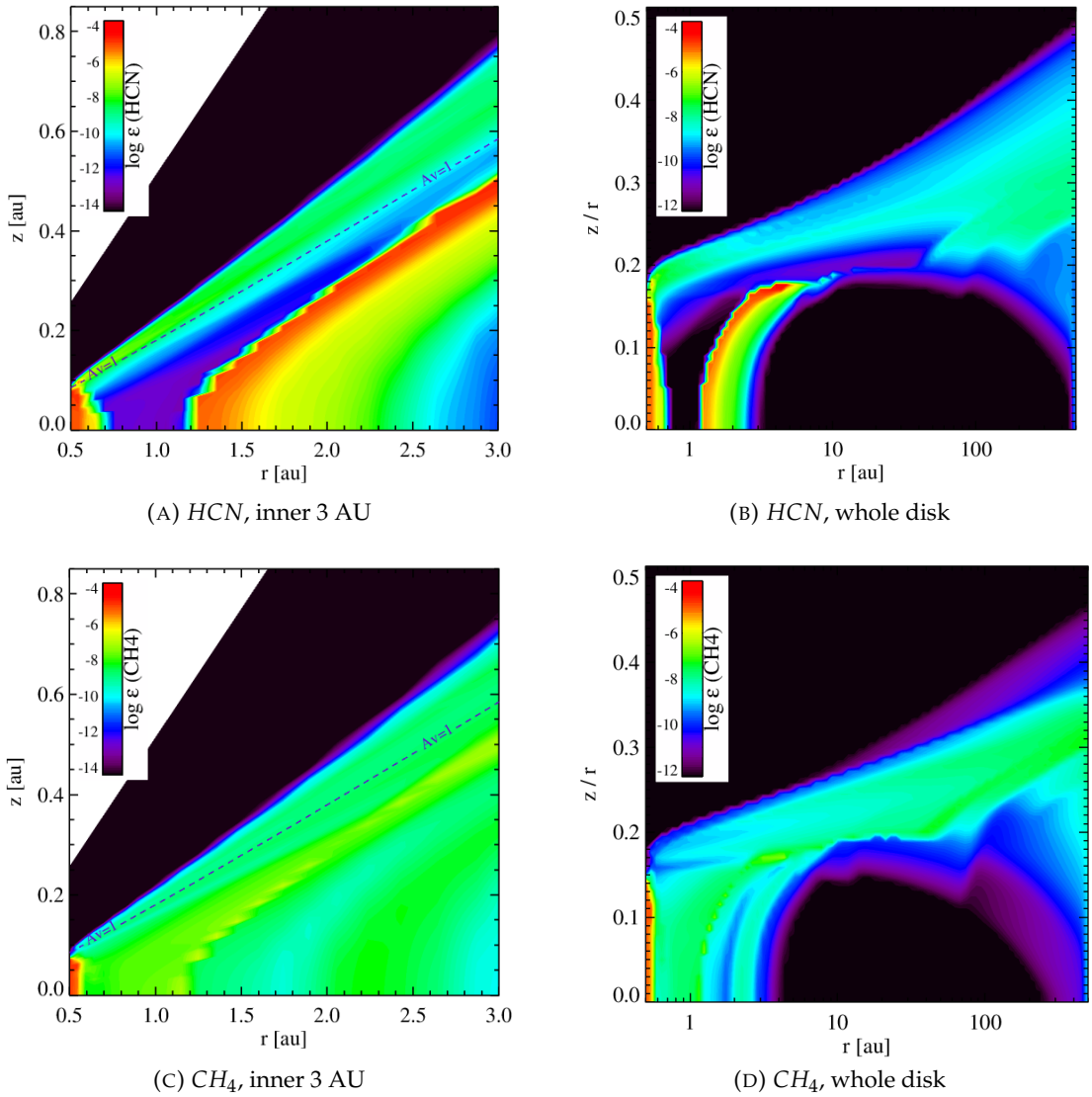

(A) HCN, inner 3 AU

(B) HCN, whole disk

(C) CH_4, inner 3 AU

(D) CH_4, whole disk

FIGURE C.2: Change in CH_4 and HCN, after changing the parameters

Appendix D

Vertical cuts at different radii

D.1 Vertical cuts of ProDiMo

D.1.1 Old parameters

The vertical cuts for the old ProDiMo model are at radius = 0.851 and 1.485 for the new ProDiMo model at R = 0.642, 0.895 and 1.475

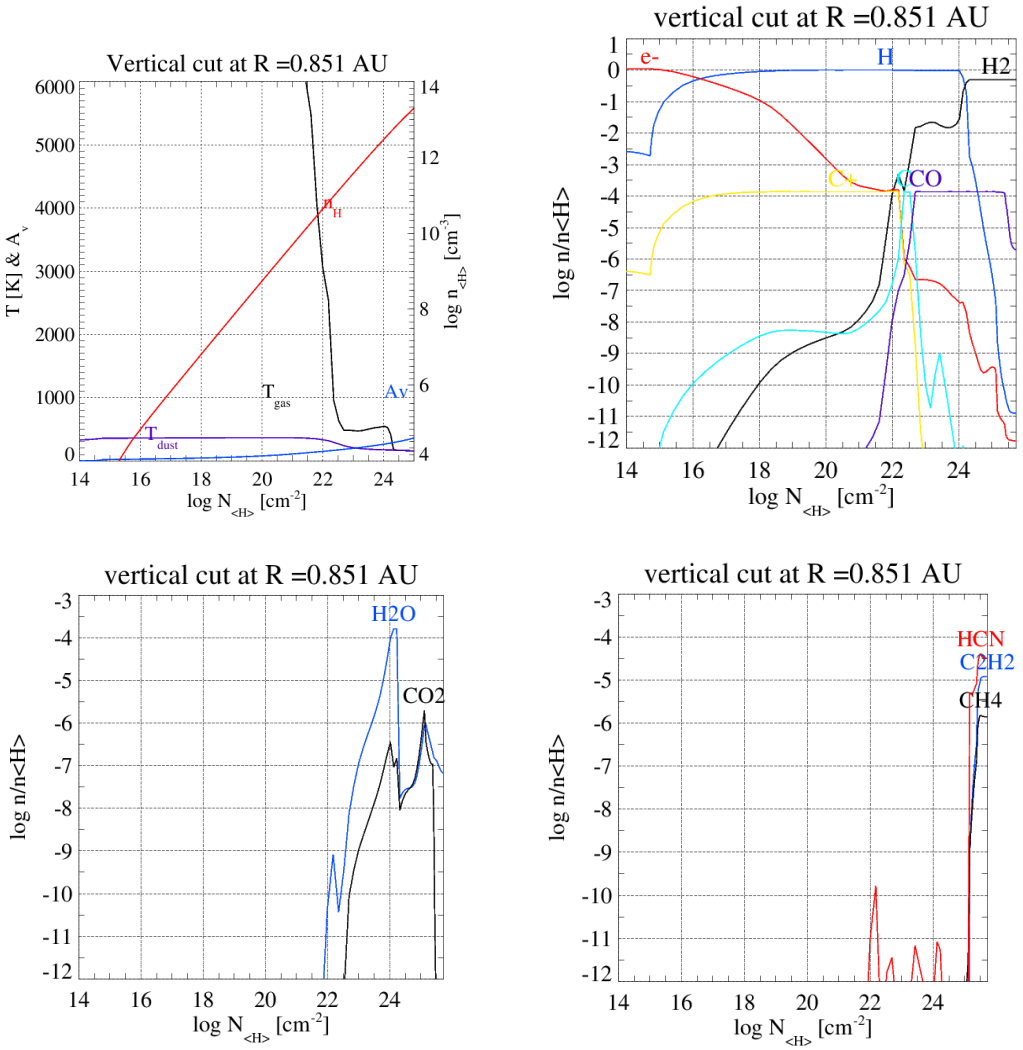

FIGURE D.1: Vertical cut at R = 0.851, plotted using the original ProDiMo so with the Parameters shown in table 2.1

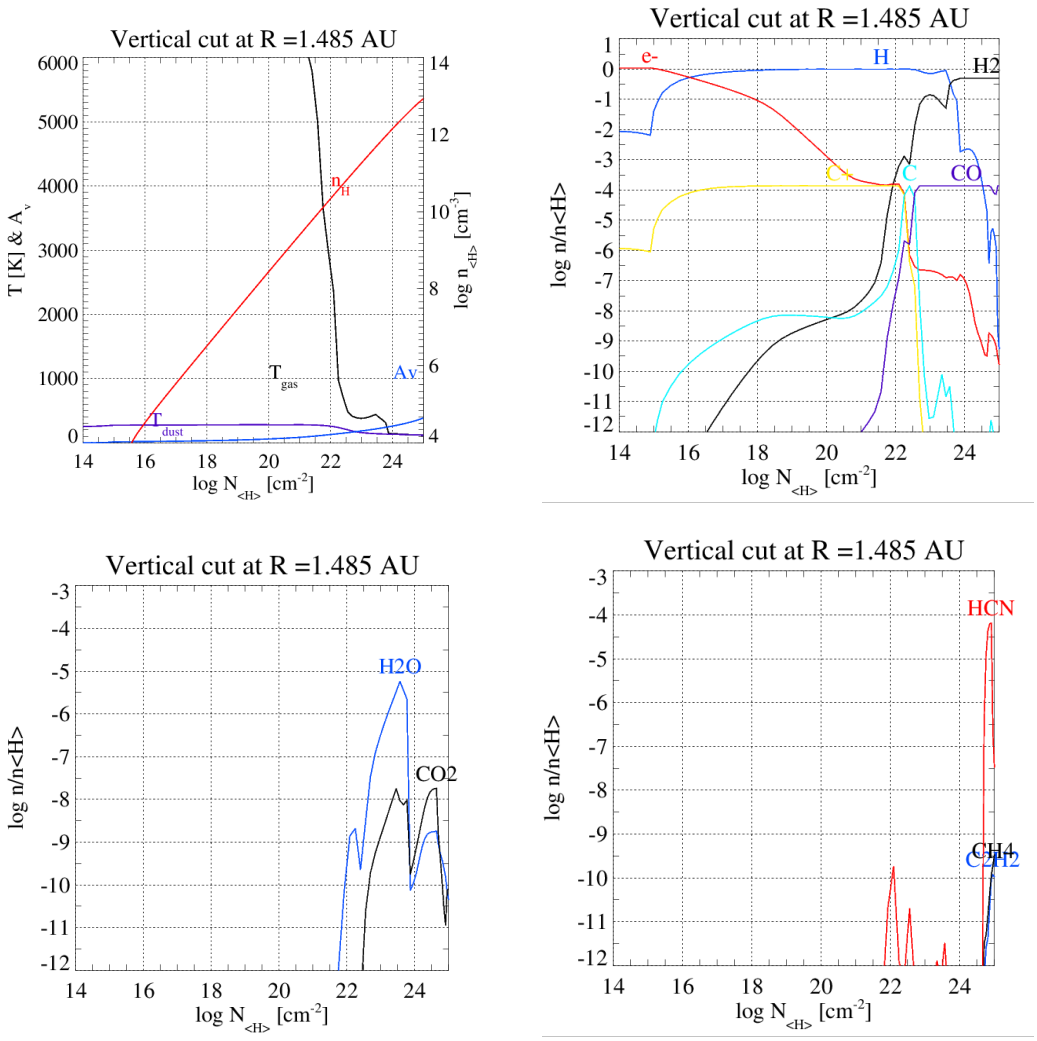

FIGURE D.2: Vertical cut at R = 1.485, plotted using the original ProDiMo so with the Parameters shown in table 2.1

D.1.2 New parameters

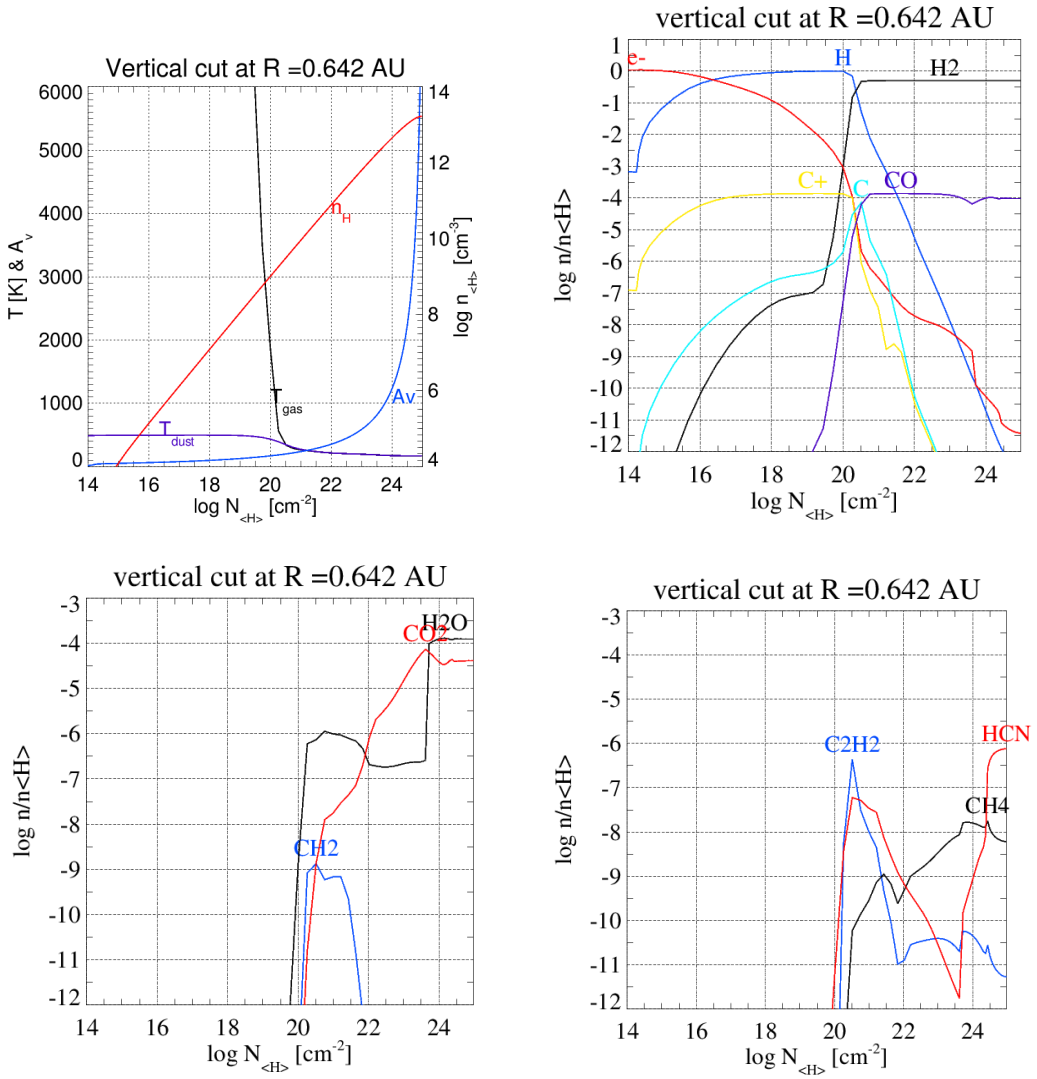

FIGURE D.3: Vertical cut at R = 0.642, plotted using ProDiMo for the model with changed parameters

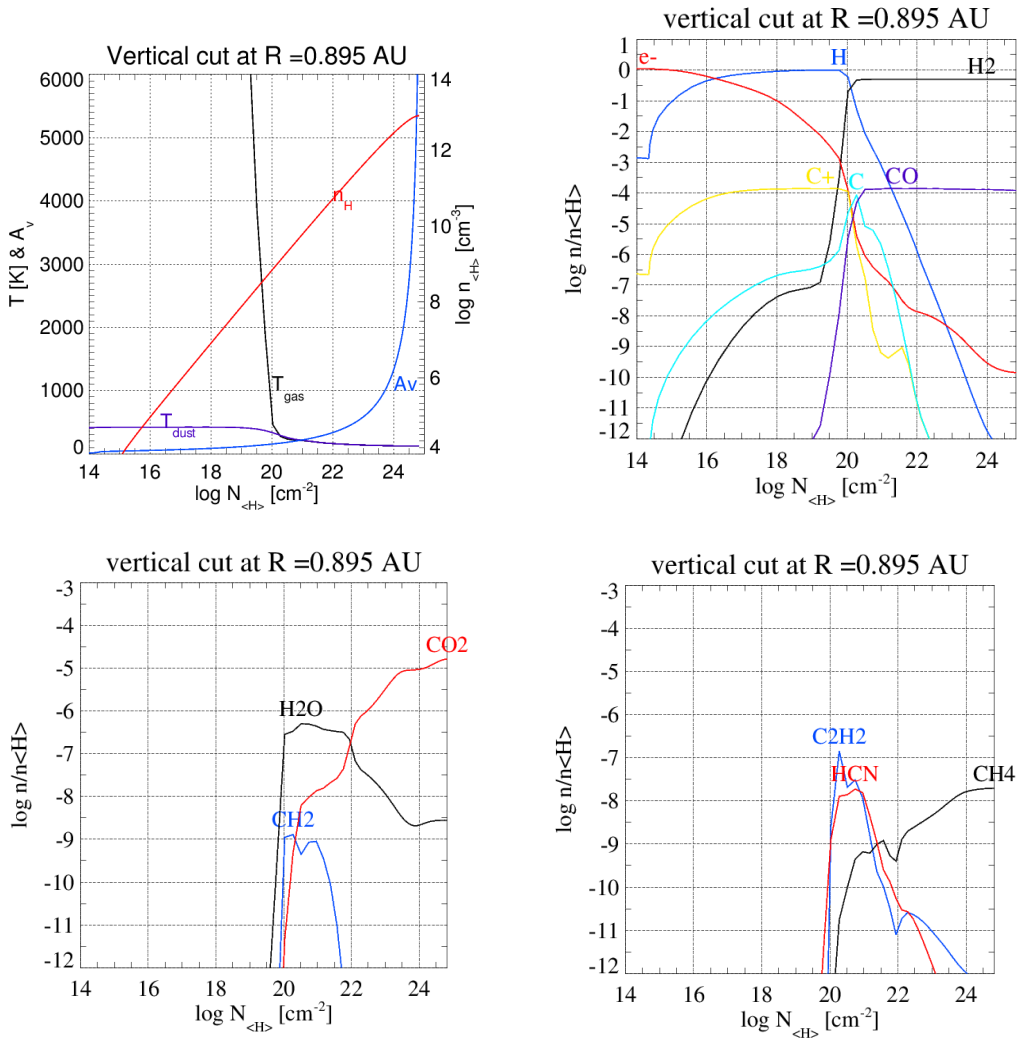

FIGURE D.4: Vertical cut around R = 0.895, plotted using ProDiMo for the model with changed parameters

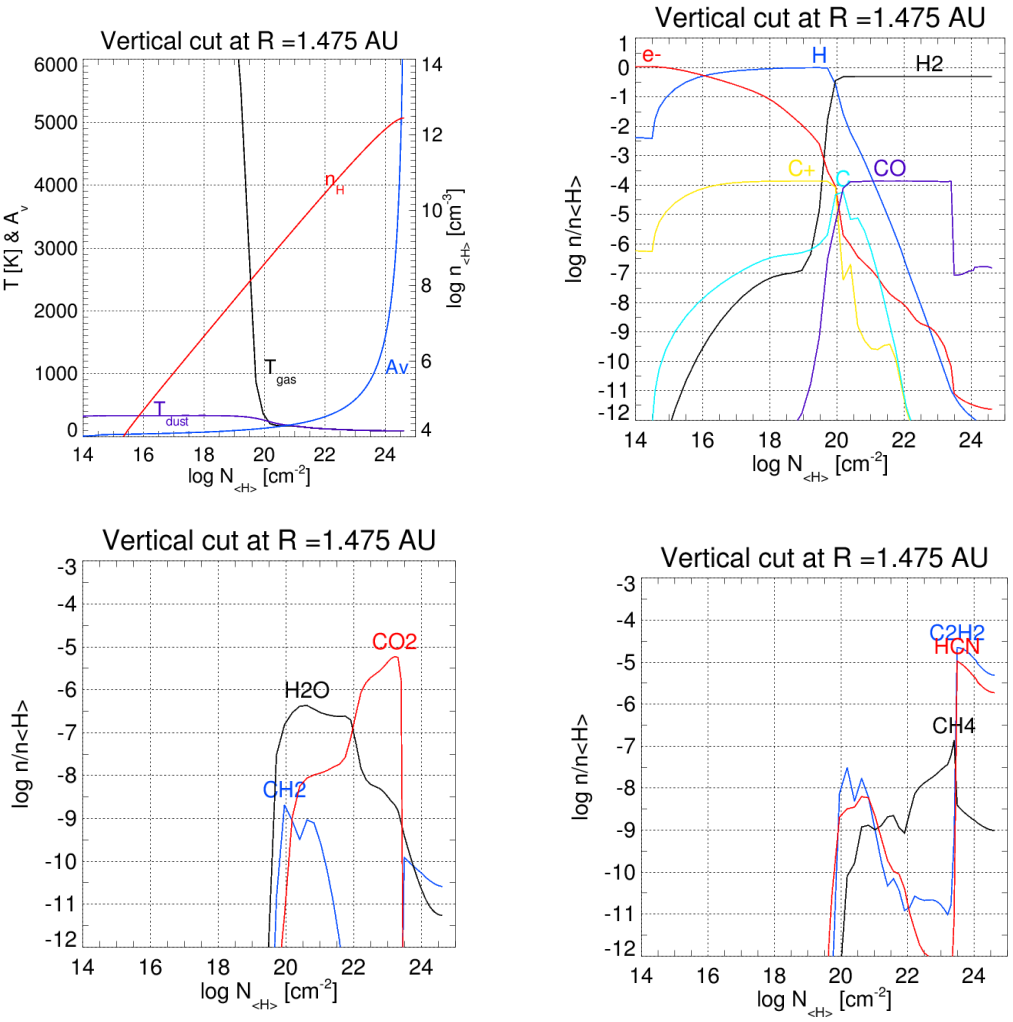

FIGURE D.5: Vertical cut at R = 1.475, plotted using ProDiMo for the model with changed parameters

D.2 Vertical cuts of Agúndez et al.

On the next four pages the vertical cut for a radius of 0.878755, 0.763209, 0.662856 and 1.544422 AU are shown, created from the data received from Marcelino Agúndez.

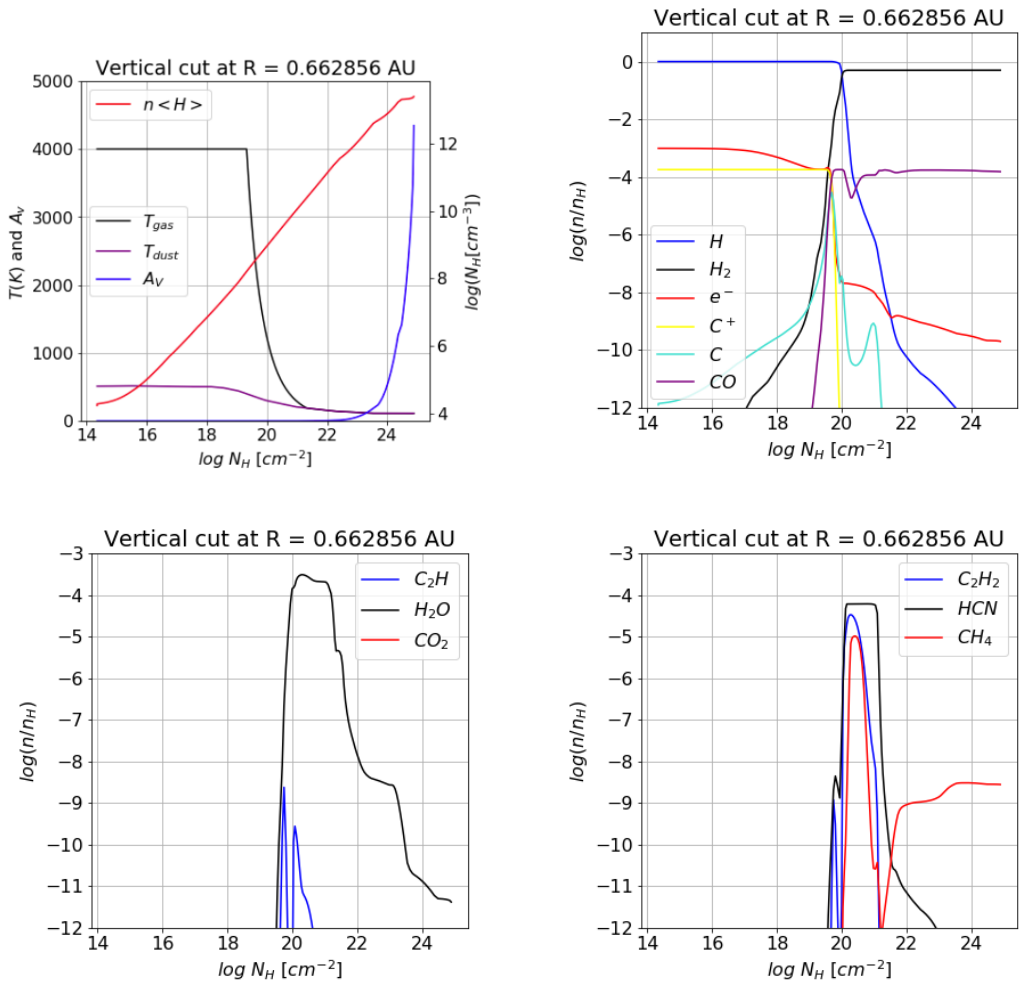

FIGURE D.6: Vertical cut at R = 0.663, constructed from the data by Agúndez et al. (2018)

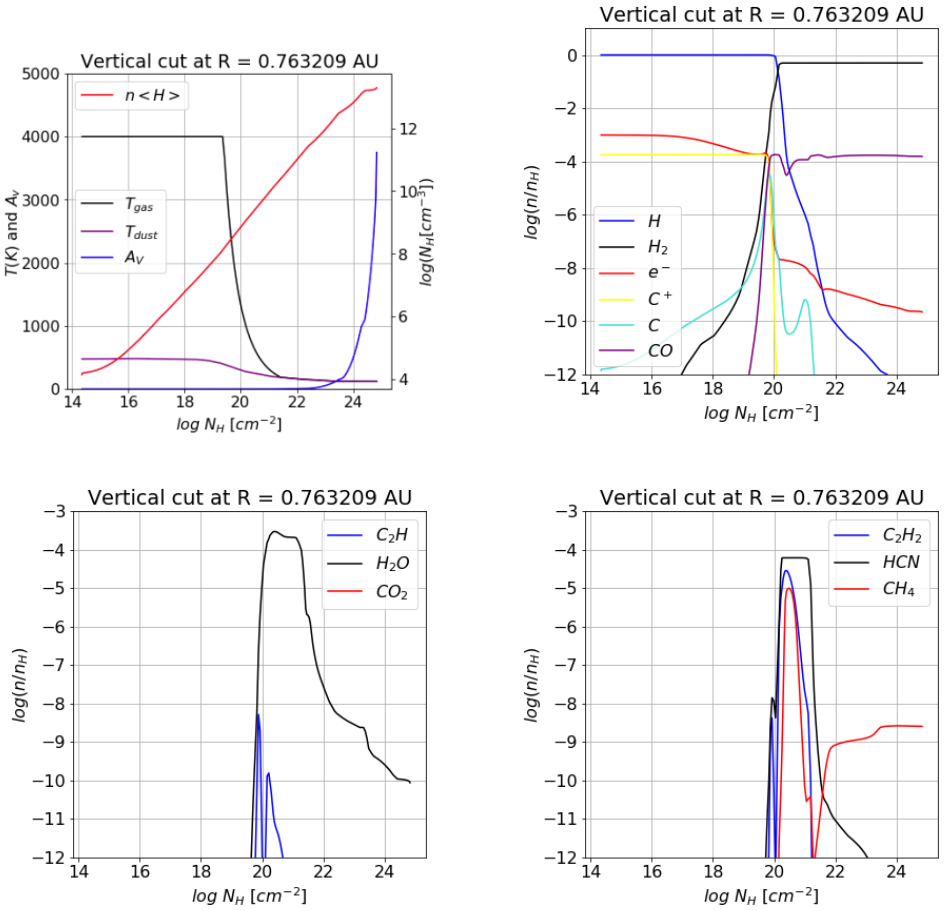

FIGURE D.7: Vertical cut at R = 0.763, constructed from the data of Agúndez et al. (2018)

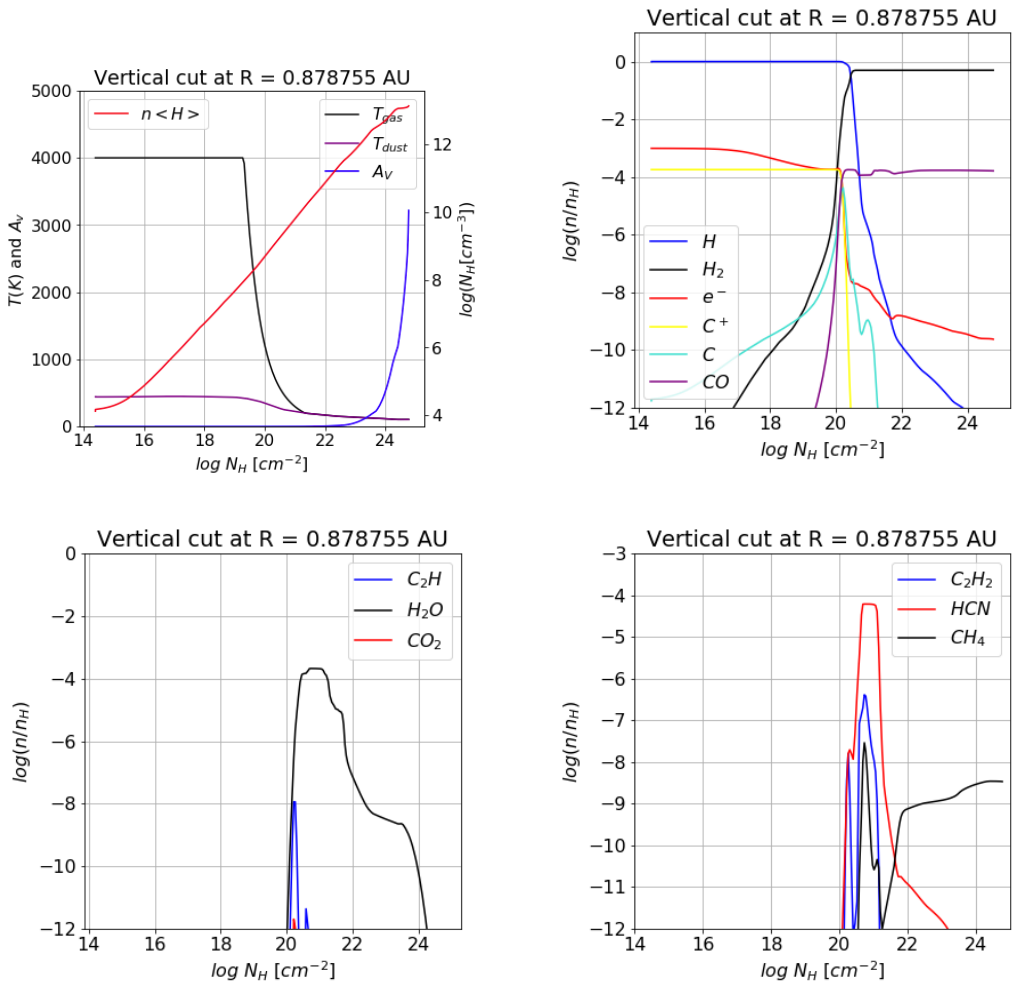

FIGURE D.8: Vertical cut at R = 0.879, constructed from the data of Agúndez et al. (2018)

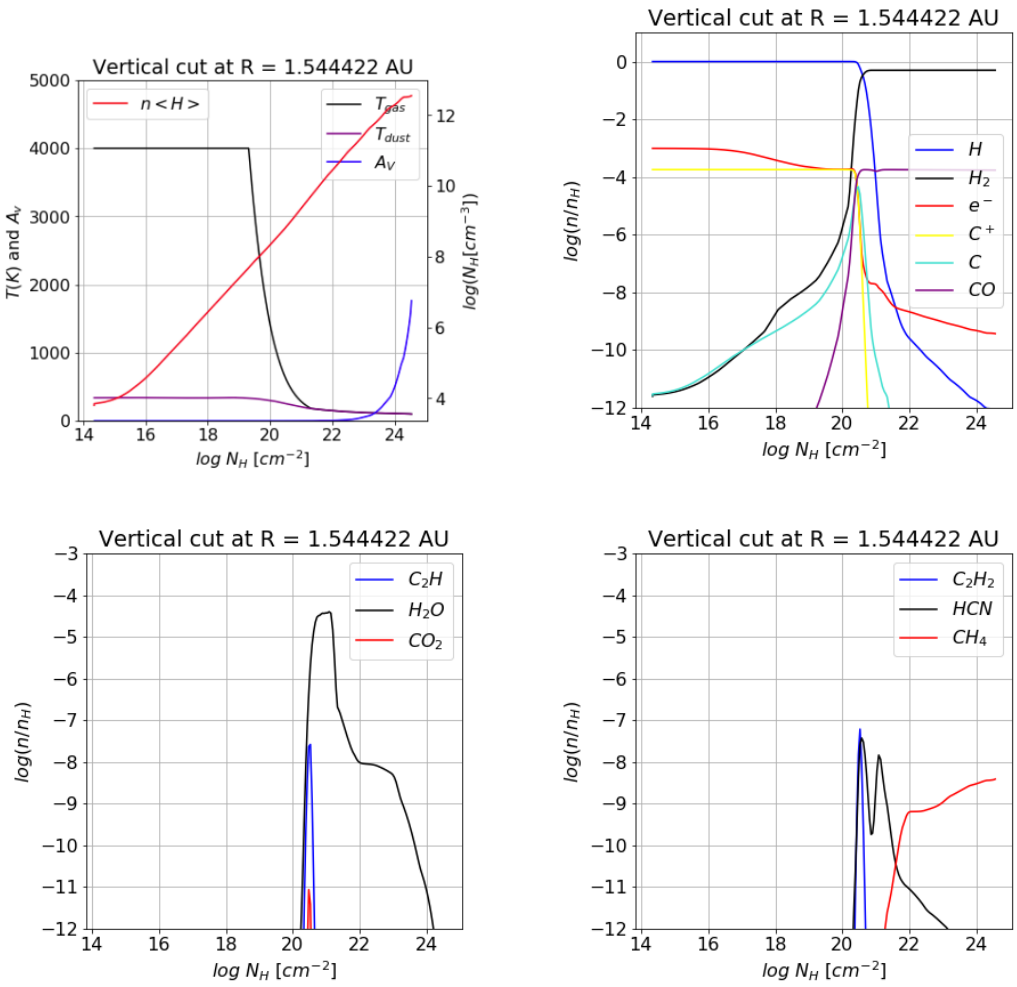

FIGURE D.9: Vertical cut at R = 1.544, constructed from the data of Agúndez et al. (2018)

Acknowledgements

For this research I'd like to thank my supervisor prof. dr. I.E.E. Inga Kamp, she helped me with the entire research but especially with understanding the code and the model. Even though she had a very busy schedule, she made a lot of time to answer my questions. The discussions, ideas, and feedback were really instructive.

I'd also like to thank Dr. Marcelino Agúndez for sharing reaction rates and data from the new model that I could use construct a vertical cut showing the species against the density. These plots really gave a good understanding of how the models are related.

I would also like to thank prof. dr. Floris van der Tak as he was kind enough to be the second reader of this thesis.

Finally, I would like thank to Dr. Christian Rab who suggested to look into the grain sizes, which turned out to solve a large part of the problem.

Bibliography

Agúndez, M. et al. (2018). "The chemistry of disks around T Tauri and Herbig Ae/Be stars". In: A&A 616, A19, A19. DOI: 10.1051/0004-6361/201732518. arXiv: 1803.09450.

Agúndez, Marcelino et al. (2008). "Formation of simple organic molecules in inner T Tauri disks". In: 483, pp. 831–837.

Cernicharo, José (2004). "The Polymerization of Acetylene, Hydrogen Cyanide, and Carbon Chains in the Neutral Layers of Carbon-rich Proto-planetary Nebulae". In: *The Astrophysical Journal Letters* 608.1, p. L41. URL: http://stacks.iop.org/1538-4357/608/i=1/a=L41.

Henning, T. and D. Semenov (2013). "Chemistry in Protoplanetary Disks". In: *Chemical Reviews* 113, pp. 9016–9042. DOI: 10.1021/cr400128p. arXiv: 1310.3151 [astro-ph.GA].

J. A. Manion R. E. Huie, R. D. Levin D. R. Burgess Jr. V. L. Orkin W. Tsang W. S. McGivern J. W. Hudgens V. D. Knyazev D. B. Atkinson E. Chai A. M. Tereza C.-Y. Lin T. C. Allison W. G. Mallard F. Westley J. T. Herron R. F. Hampson and D. H. Frizzell (2018). *NIST Chemical Kinetics Database*. URL: http://kinetics.nist.gov (visited on 10/24/2018).

Lahuis, F. et al. (2006). "Hot Organic Molecules toward a Young Low-Mass Star: A Look at Inner Disk Chemistry". In: *The Astrophysical Journal Letters* 636.2, p. L145. URL: http://stacks.iop.org/1538-4357/636/i=2/a=L145.

Le Teuff, Y. H., T. J. Millar, and A. J. Markwick (2000). "The UMIST database for astrochemistry 1999". In: A&AS 146, pp. 157–168. DOI: 10.1051/aas:2000265.

McElroy, D. et al. (2013). "The UMIST database for astrochemistry 2012". In: *A&A* 550, A36. DOI: 10.1051/0004-6361/201220465. URL: https://doi.org/10.1051/0004-6361/201220465.

Salyk, C. et al. (2011). "A Spitzer Survey of Mid-infrared Molecular Emission from Protoplanetary Disks. II. Correlations and Local Thermal Equilibrium Models". In: *The Astrophysical Journal* 731.2, p. 130. URL: http://stacks.iop.org/0004-637X/731/i=2/a=130.

Woitke, P. et al. (2016). "Consistent dust and gas models for protoplanetary disks. I. Disk shape, dust settling, opacities, and PAHs". In: A&A 586, A103, A103. DOI: 10.1051/0004-6361/201526538. arXiv: 1511.03431 [astro-ph.EP].

Woitke, P., Kamp, I., and Thi, W.-F. (2009). "Radiation thermo-chemical models of protoplanetary disks - I. Hydrostatic disk structure and inner rim". In: *A&A* 501.1, pp. 383–406. DOI: 10.1051/0004-6361/200911821. URL: https://doi.org/10.1051/0004-6361/200911821.

Woodall, J. et al. (2007). "The UMIST database for astrochemistry 2006*". In: *A&A* 466.3, pp. 1197–1204. DOI: 10.1051/0004-6361:20064981. URL: https://doi.org/10.1051/0004-6361:20064981.

Woods, Paul M. and Karen Willacy (2007). "Benzene Formation in the Inner Regions of Protostellar Disks". In: *The Astrophysical Journal Letters* 655.1, p. L49. URL: http://stacks.iop.org/1538-4357/655/i=1/a=L49.